

Structure-based discovery of a new selectivity-enabling motif for the FK506-binding protein 51

Fabian H. Knaup¹, Christian Meyners¹, Wisely Oki Sugiarto¹, Saskia Wedel², Margherita Springer³, Carlo Walz¹, Thomas M. Geiger¹, Mathias V. Schmidt³, Marco Sisignano^{2,4}, Felix Hausch^{1}*

¹Department of Chemistry and Biochemistry Clemens-Schöpf-Institute, Technical University Darmstadt, Alarich-Weiss Straße 4, 64287 Darmstadt, Germany.

²Pharmazentrum Frankfurt/ZAFES, Institute of Clinical Pharmacology, University Hospital, Theodor-Stern-Kai 7, 60590 Frankfurt am Main, Germany

³Research Group Neurobiology of Stress Resilience, Max Planck Institute of Psychiatry, 80804 Munich, Germany.

⁴Fraunhofer Institute for Translational Medicine and Pharmacology ITMP, Theodor-Stern-Kai 7, 60596 Frankfurt am Main

KEYWORDS: FKBP51, FKBP5, bioisoster, transient binding pocket, induced fit, SAFit

ABSTRACT

In recent years the selective inhibition of FKBP51 has emerged as a possible treatment for chronic pain, obesity-induced diabetes, or depression. All currently known advanced FKBP51-selective inhibitors, including the widely used SAFit2, contain a cyclohexyl residue as a key motif for enabling selectivity over the closest homolog and anti-target FKBP52. During a structure-based SAR exploration we surprisingly discovered thiophenes as highly efficient cyclohexyl replacement moieties that retain the strong selectivity of SAFit-type inhibitors for FKBP51 over FKBP52. Cocrystal structures revealed that the thiophene-containing moieties enable selectivity by stabilizing a flipped-out conformation of Phe⁶⁷ of FKBP51. Our best compound **19b** potently binds to FKBP51 biochemically as well as in mammalian cells, desensitize TRPV1 in primary sensory neurons, and has an acceptable PK profile in mice, suggesting its use as novel tool compound for studying FKBP51 in animal models of neuropathic pain.

INTRODUCTION

The FK506-binding protein 51 (FKBP51, encoded by the FKBP 5 gene) is a cochaperone of the Hsp90 machinery and binds the natural products FK506 and Rapamycin.¹ FKBP51 plays a prominent role in mammalian stress biology. Its expression is robustly induced by various stressful stimuli in cells, animals and humans.²⁻⁴ FKBP51 is a suppressor of stress hormone receptors, making FKBP51 the key factor in an ultrashort negative feedback loop positioned to fine-tune stress responses.^{5,6} In recent years it has become evident that dysregulation of FKBP51 is associated with the development of several stress-related diseases and mental disorders⁷⁻¹⁰, as well as being a risk factor for obesity¹¹⁻¹³ and chronic pain.^{9,14-16} Therefore, inhibiting FKBP51 represents a mechanistically novel approach for treating these diseases.¹⁷⁻¹⁹

Selective inhibition of FKBP51 is challenging due to its close homolog FKBP52, which has a highly conserved binding site but opposite biological effects compared to FKBP51.²⁰⁻²² FKBP51 can be selectively addressed by targeting a transient binding pocket, defined by the Phe67^{out} conformation, which is highly disfavored for FKBP52. All known advanced FKBP51-selective ligands, including the widely used SAFit2 and newly developed macrocycles, use a cyclohexyl group as the Phe67^{out}-stabilizing moiety (crucial for selectivity) and a D⁶⁸/S¹¹⁸/K¹²²-targeting trialkoxyaryl-moiety to achieve potency (Figure 1).²³⁻²⁶ Especially the cyclohexyl group was shown to be very sensitive to minor modifications and despite substantial efforts, all attempts to replace this group were not met with success.^{24,27,28}

Here, by a surprising flip of the D⁶⁸/S¹¹⁸/K¹²²-vs F⁶⁷-targeting moieties, we identified chlorothiophens as the first useful cyclohexyl mimics that robustly enable highly potent and selective FKBP51 inhibitors based on a novel scaffold.

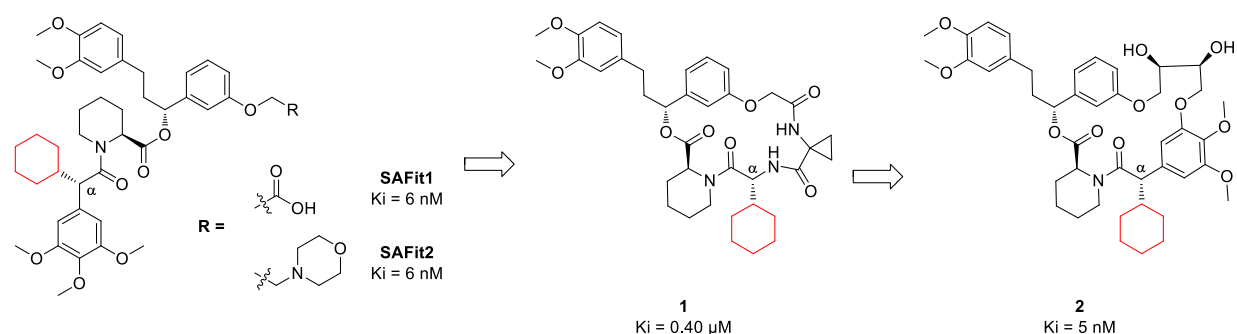


Figure 1: Chemical structures and binding affinities for FKBP51 of **SAFit1/2**, and the recently discovered macrocyclic inhibitors **1** and **2**. The selectivity enabling cyclohexyl group is highlighted in red.

RESULTS AND DISCUSSION

Identification of a novel motif for the selective inhibition of FKBP51

In this study, we initially aimed to find a suitable replacement for the 3,4,5-trimethoxyphenyl residue of **SAFit1**. This residue is beneficial for the high binding affinity towards FKBP51 but also contributes to the poor pharmacological properties due to its electron-rich nature (Figure 2).²⁹

In previous SAR studies, the methoxy groups of the 3,4,5-trimethoxyphenyl residue have been systematically removed, revealing a surprisingly strong effect of the three methoxy groups.²⁵ Furthermore, the phenyl moiety was substituted by smaller alkyl chains containing different functional groups, such as chiral alcohols, ethers, and ketones.²⁵ Overall, however, none of those ligands rivalled the affinity of **SAFit1**. Therefore, we considered a bioisosteric replacement of the phenyl ring of compound **3** to replace the electron-rich 3,4,5-trimethoxyphenyl moiety. We opted for thiophenes and were delighted to see that the affinity for FKBP51 was retained for **4a** and even increased for **4b** compared to compound **3** (Figure 2). Moreover, the selectivity vs FKBP52 was retained for **4a** and **4b** ($K_i^{\text{FKBP52}} > 10 \mu\text{M}$).

Initially, compounds **4a** and **4b** were synthesized and tested as a diastereomeric mixture. For all SAFit analogs studied so far, affinity for FKBP51 was associated with the cyclohexyl-bearing carbon ($C\alpha$) being in the (S)-configuration. We therefore assumed the corresponding $C\alpha$ -(S) diastereomers of **4a** and **4b** to account for the observed binding to FKBP51.

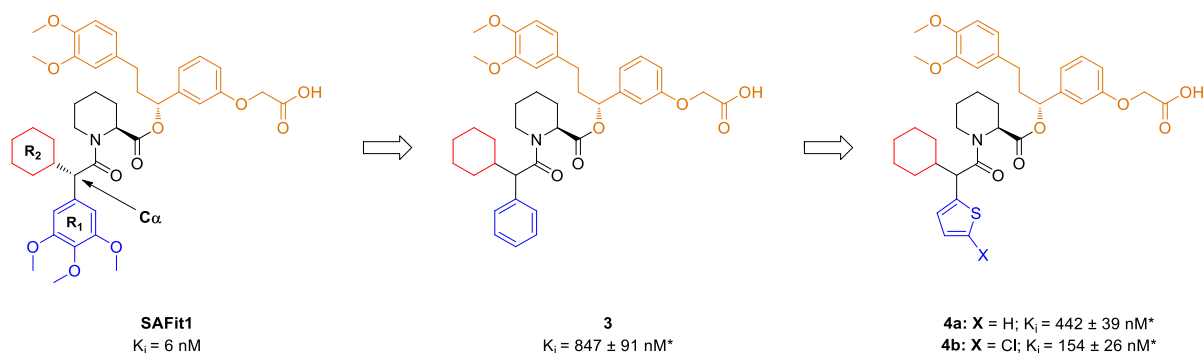


Figure 2: Chemical structures of SAFit1, compounds **3***, **4a***, **4b*** and their binding affinities towards FKBP51. FKBP51 selective inhibitors contain a top group (orange), a pipercolic core (black) and bottom group. The bottom group is composed of a selectivity-inducing cyclohexyl residue (R_2 , red) and a trimethoxyaryl moiety (R_1 , blue). *measured as mixture of diastereomers (R/S at $C\alpha$).

To investigate the molecular interactions of the newly introduced (5-chloro)thiophene group with FKBP51, we determined the cocrystal structures of (**R/S**)**4a** and (**R/S**)**4b** in complex with FKBP51 (Figure 3B & C).³⁰ For both compounds, the pipercolate and the attached ‘top’ group engaged FKBP51 in a SAFit-like manner, incl. the displacement of Phe⁶⁷ to the out-conformation as the basis for selectivity vs FKBP52. To our great surprise, however, we only observed the $C\alpha$ -(*R*)-diastereomer of **4a** and **4b** in complex with FKBP51, although both diastereomers were present at equal concentrations in the crystallization mixture. In both crystal structures, the thienyl moieties of **4a** and **4b** are buried deep inside the transient hydrophobic pocket, which forms upon the outward flip of Phe⁶⁷. The thienyl groups roughly adopt a position previously occupied by the

cyclohexyl group in SAFit-like compounds. Conversely, the cyclohexyl groups of **4a** and **4b** adopted positions previously occupied by the 3,4,5-trimethoxyaryl moiety. Overall, this observation led to the hypothesis that the thiophene residue is a promising cyclohexyl mimetic that can induce selectivity over FKBP52.

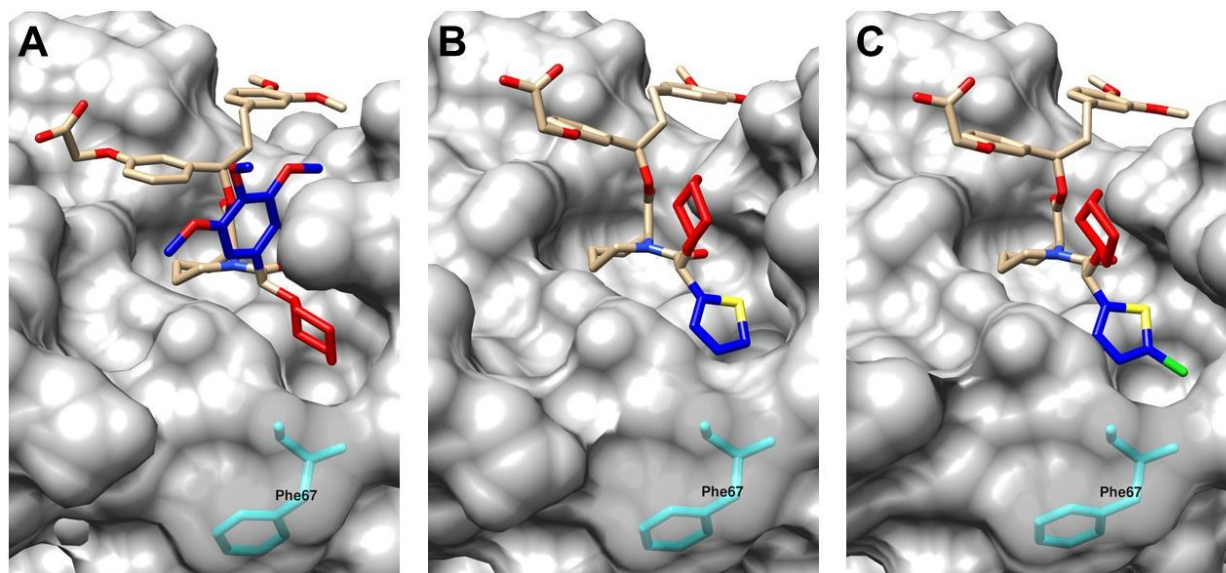
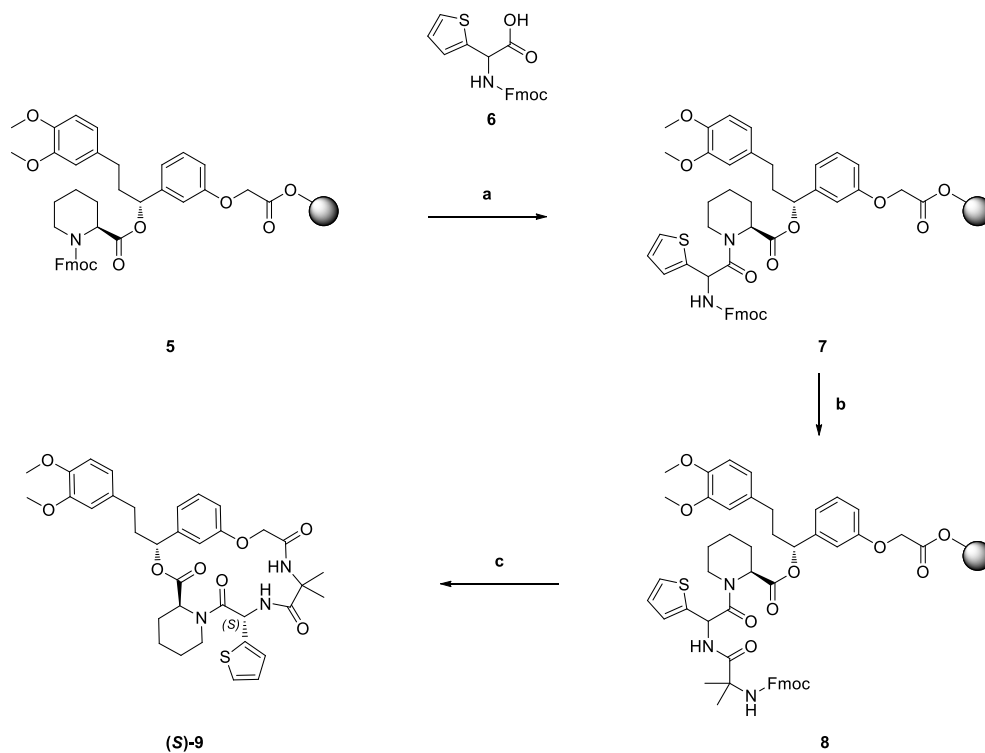


Figure 3: Co-crystal structure of SAFit- analogs (sticks) in complex with the FK1 domain of FKBP51 (grey surface, the displaced Phe⁶⁷ highlighted in cyan). The cyclohexyl moiety is shown in red, the aryl moieties are shown in blue, and the rest of the ligand are shown in pale orange. (A) Co-crystal structure of SAFit1 (PDB: 8CCA). (B) Co-crystal structure of compound **4a** (PDB: 8CCH). (C) Co-crystal structure of compound **4b** in complex with FKBP51 (PDB: 8CCB).

We recently discovered SAFit-derived macrocycles as a promising scaffold to position side chains such as the cyclohexyl moiety poised for binding to FKBP51 (Figure 1, compound **1**).²⁸ To explore if the here discovered thiophene moiety would also work in a rigidified macrocyclic context, we synthesized compound **9**, starting from building block **5** and Fmoc protected (2-thiophene)glycine (Scheme 1). The obtained pair of diastereomers was separated by preparative HPLC, yielding the diastereomeric pure compounds (*S*)-**9** and (*R*)-**9**. Notable, during the determination of the binding

affinities for FKBP51 and FKBP52 by FP assay, only one of the obtained diastereomers showed a measurable binding affinity for FKBP51 (0.8 μM) and selectivity over FKBP52 (>50 μM). Therefore, we assumed that this diastereomer contains the correct (*S*)-configuration in the $\text{C}\alpha$ -position of the amide bond.

Scheme 1: Synthesis of the thiophene-containing macrocycle (*S*)-**9**.



Reagents and conditions: a) 1. 20 vol.-% 4-methylpiperidine in DMF, rt; 2. **6**, HATU, HOAt, DIPEA, DMF, rt; b) 1. 20 vol.-% 4-methylpiperidine in DMF, 0°C; 2. Fmoc-Aib-OH, HATU, HOAt, DIPEA, DMF, rt; c) 1. 20 vol.-% HFIP in DCM, rt; 2. HATU, DIPEA, DMF, rt.

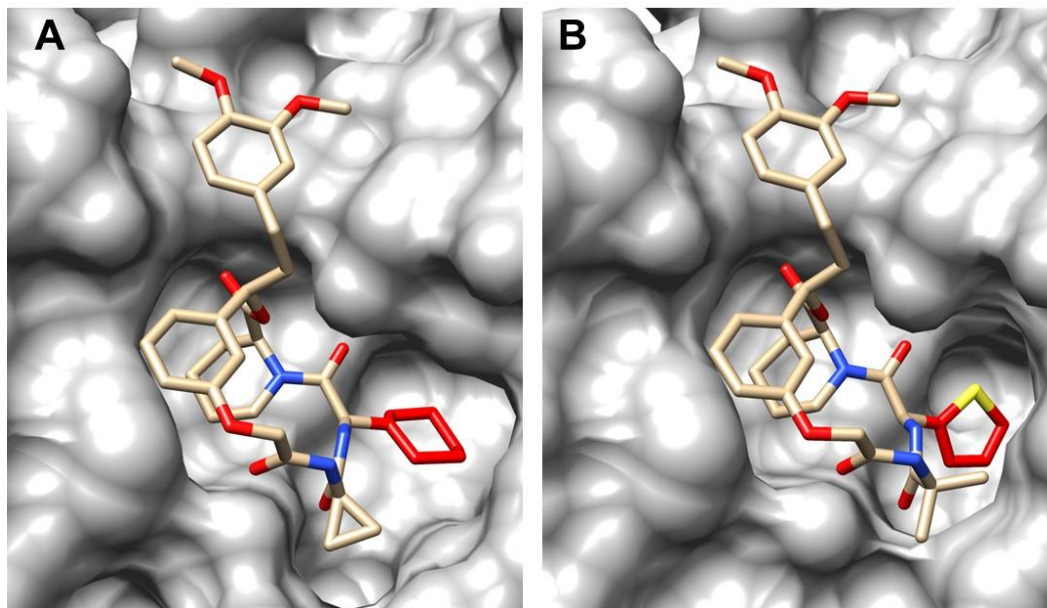


Figure 4: Comparison of the co-crystal structures of compounds **1** and (*S*)-**9**. The selectivity-inducing cyclohexyl and 2-thienyl moiety is shown in red and the rest of the ligands is shown in pale orange. (A) Co-crystal structure of **1** in complex with the FK1 domain of FKBP51 (PDB: 7AOU). (B) Co-crystal structure of (*S*)-**9** in complex with the FK1 domain of FKBP51 (PDB: 8CCG).

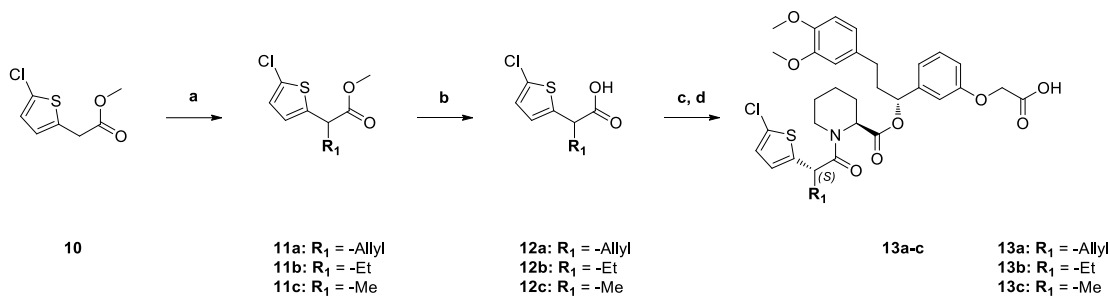
To further validate this, we obtained the high-resolution co-crystal structure of compound (*S*)-**9** in complex with the FK1 domain of FKBP51 (Figure 4B). The comparison of the co-crystal structure of compound **1** (Figure 4A) and (*S*)-**9** indicates that the overall binding mode of both macrocyclic ligands is very similar. Furthermore, the thiophene group is located in the transient binding pocket, which is crucial for the selectivity towards FKBP51.

Structure-affinity relationship (SAR) of chlorothiophene-containing moieties

To understand the role of the cyclohexyl group in the new binding mode, we synthesized compounds **13a-c** as pure (*S*)-configured diastereomers, where the size of the C α -substituent was systematically reduced from allyl to methyl group. Towards this end, the racemic carboxylic acids **12a-c** were synthesized by alkylation of ester **10**, followed by cleavage of the methyl ester (Scheme 2). Subsequent HATU coupling with the immobilized core-/top group **5** and subsequent

cleavage of the products from the solid support resulted in diastereomeric mixtures, which were separated via preparative HPLC, yielding the diastereomeric pure compounds **(S)-13a-c** and **(R)-13a-c**.

Scheme 2: Synthesis of 5-chlorothiophene-containing compounds (S)-13a-c and (R)-13a-c.



Reagents and conditions: a) LiHMDS, R₁-X (for **11a**: AllylBr, for **11b**: EtI and for **11c**: MeI), reTHF, -78°C – rt. b) LiOH, THF/MeOH/H₂O (3:1:1), rt. c) 1. **5**, 4-methylpiperidine, DMF, 0°C 2. **12a-c**, HATU, HOAt, DIPEA, DMF, rt. d) 20 vol.-% HFIP in DCM, rt.

Table 1: Overview of binding affinities of the SAFit1 analogs (S)-13a-c.

Entry	R ₁	FKBP51 K _i [nM]	FKBP52 K _i [nM]
4b*		154 ± 26*	> 30,000*
13a		223 ± 19	> 10,000
13b		210 ± 11	> 10,000
13c		300 ± 25	> 50,000

*Tested as a diastereomeric mixture.

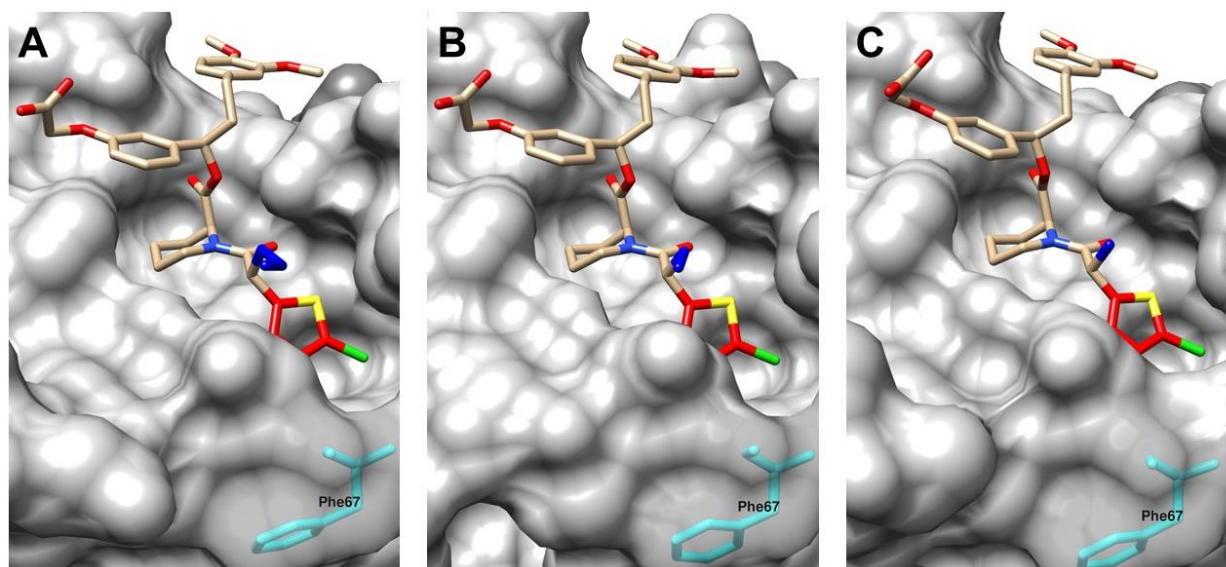


Figure 5: Comparison of the co-crystal structures of compounds (**S**)-**13a-c**. (A) Co-crystal structure of the FK1 domain of FKBP51 in complex with (**S**)-**13a** (A, PDB: 8CCF), (**S**)-**13b** (B, PDB: 8CCE), and (**S**)-**13c** (C, PDB: 8CCC).

The binding affinities of compounds (**S**)-**13a-c** and (**R**)-**13a-c** for FKBP51 and FKBP52 were determined by fluorescent polarization assay.³¹ For all diastereomeric pairs, only one compound bound to FKBP51 with high affinity (Table 1 and SI Table 1). These were tentatively assigned as the $C\alpha$ -(**S**) diastereomers. Truncation of the cyclohexyl group in the context of a chlorothiophene group only marginally reduced affinity to FKBP51 and the smallest analog (**S**)-**13c** (R=Me) still retained appreciable binding (300nM). Notable, compounds (**S**)-**13a-c** all showed moderate binding affinities for FKBP51, while retaining high selectivity for FKBP51 over FKBP52. To confirm the binding mode of (**S**)-**13a-c** and to understand the interactions of the alkyl in R₁ with FKBP51, we obtained the high-resolution co-crystal structures of compounds (**S**)-**13a-c** in complex with FKBP51 (Figure 5). The crystal structures clearly showed that (i) (**S**)-**13a-c** have the correct stereochemistry, (ii) the 5-chlorothiophenes bind to the transient binding pocket resulting from displacement of Phe⁶⁷, (iii) the alkyl groups engage in hydrophobic interactions with Ile¹²² and are partially solvent-exposed.

Taken together, the cyclohexyl group is dispensable in the context of a 5-chlorothiophene group, and a simple methyl group seems sufficient to induce selective inhibition of FKBP51 with a moderate binding affinity.

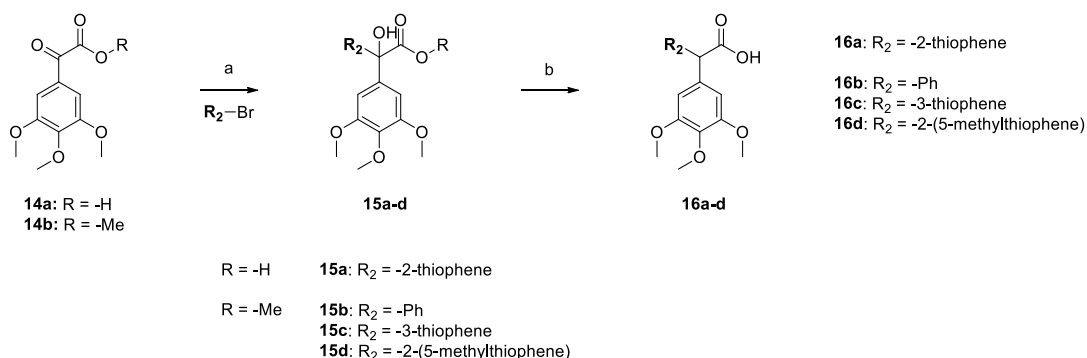
Exploration of the thiophene moiety

Given that the 3,4,5-trimethoxyphenylacetic acids is a highly preferred subgroup in the context of cyclohexyl-containing SAFit analogs, we explored if this subgroup is compatible with the newly discovered thiophene moiety. Towards this goal, it was a new synthesis had to be established, which also allowed for a further exploration of the thiophene moiety itself (Scheme 3).

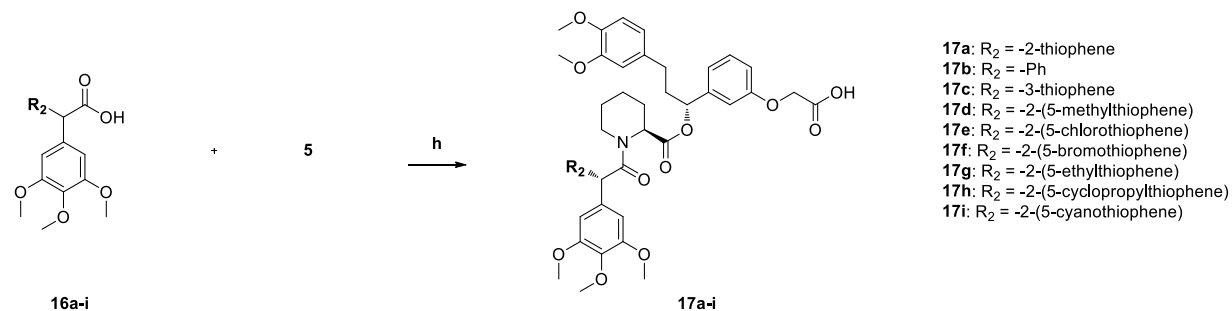
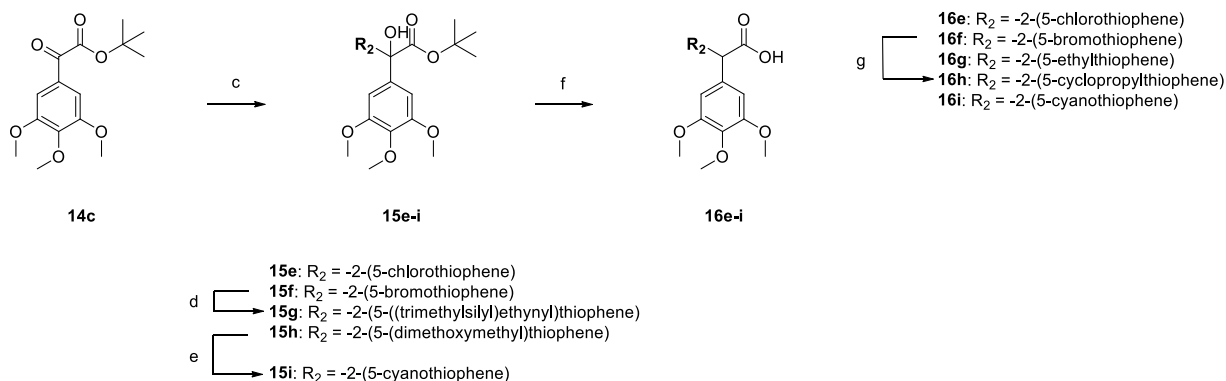
The synthesis started from the α -ketoacid **14a** or methyl- α -ketoacid ester **14b** (Route A), which were reacted with different aryl-/ heteroaryl organolithium reagent or Grignard reagents to yield compounds **15a-d**. After deoxygenation of the hydroxy group using triethylsilane and catalytical amounts of InCl_3 , followed by ester hydrolysis for the methyl ester analogs **15b-d**, the 2-substituted 3,4,5-trimethoxyphenylacetic acids **16a-d** were obtained. Since not all formed organolithium reagents were stable at room temperature, we were forced to add the ester to the formed organolithium reagent. We further increased the bulk of the ester group by using the tertbutyl ester **14c** to avoid side reactions at the methyl ester. This optimized procedure (Scheme 3, Route B) provided the α -hydroxy esters **15e-i** in good yields.

Scheme 3: Synthesis of 3,4,5-trimethoxyphenyl-containing thiophene analogs **17a-i**.

Route A:



Route B:

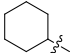
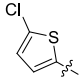
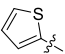
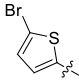
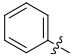
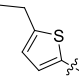
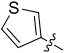
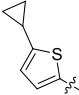
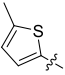
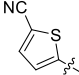


Reagents and conditions: a) for **15a**, **15c**: R₂-Br, iPrMgCl LiCl, THF 0°C – rt; for **15b**: PhLi, THF, -78°C; for **15d**: R₂-Br, tertBuLi, THF, -78°C; b) for **16a**: InCl₃, Et₃SiH, DCM, rt; for **16b–d**: 1. InCl₃, Et₃SiH, DCM, rt; 2. LiOH, THF/MeOH/H₂O (3:1:1), rt; c) R₂-Br, nBuLi, diethylether, -78°C; d) Trimethylsilylacetylene, Pd(dppf)Cl₂, CuI, Et₃N, 75°C; e) I₂, 28 wt.-% NH₃(aq.), THF, rt; f) Et₃SiH, TFA/DCM, rt; for **16i**: Ph₂SiHCl, InCl₃, DCM, rt; g) cyclopropylboronic acid, Pd(OAc)₂, SPhos, K₃PO₄, toluene/H₂O (20:1), 100°C. h) 1. **5**, 4-methylpiperidine, DMF, 0°C 2. for **17a**, **17d**, **17e**: trichloroacetonitrile, PPh₃, DIPEA, DCM, rt; for

17b: COMU, pyridine, DMF, rt; for **17c**: T3P, pyridine, DMF, rt; for **17f-h**: oxalyl chloride, DIPEA, DCM, 0°C – rt; for **17i**: TCFH, NMI, DCM/MeCN, rt. 3. 20 vol.-% HFIP in DCM, rt.

After the deoxygenation of compounds **15e-i** and deprotection of the tert butyl ester in one step, the carboxylic acids **16e-i** were obtained and coupled to the immobilized SAFit1 core/top group **5**. Afterwards, the obtained diastereomeric mixtures were separated via preparative HPLC, and the binding affinity was determined by a fluorescence polarization assay. Gratifyingly, all analogs display medium to high affinity for FKBP51 (<150nM). Again, for all diastereomeric pairs, only one of the analogs was active, while the other diastereomer did not bind (>10μM, SI Table 1).

Table 2: Overview of the binding affinities of SAFit1 and the analogs **17a-i**.

Entry	R ₂	FKBP51 K _i [nM]	FKBP52 K _i [nM]	Entry	R ₂	FKBP51 K _i [nM]	FKBP52 K _i [nM]
SAFit1		6 ± 0.4	3859 ± 2395	17e		4 ± 1	950 ± 215
17a		103 ± 12	10171 ± 923	17f		7 ± 1	436 ± 56
17b		118 ± 9	43792 ± 9206	17g		13 ± 1	>1,000
17c		140 ± 19	17951 ± 2463	17h		41 ± 5	>1,000
17d		7 ± 1	1030 ± 286	17i		23 ± 3	2728 ± 332

The 2- or 3-thiophenes (**17a** or **17c**) themselves turned out to be moderate bioisosteric replacement for the cyclohexyl group in this series and were similar to a simple phenyl ring (**17b**) (Table 2). Encouraged by these findings we next explored different substituted 2-thienyl analogs further. Upon substitution in the 5-position of the 2-thienyl moiety with a methyl group (**17d**), chlorine (**17e**), and bromine atom (**17f**), binding affinities improved dramatically to the single-digit

nanomolar range, representing a >25-fold improvement compared to compound **17a**. Slightly larger substituents such as a nitrile, ethyl or cyclopropyl group in the 5-position of the 2-thiophene were also accepted, leading to affinities between 10-50nM. All thiophene analogs were selective vs FKBP52, binding approximately 100-fold better to FKBP51 compared to FKBP52. However, the selectivity slight decreased compared to SAFit1.

To confirm the binding mode of this series, the active diastereomer of **17e** as the best representative was co-crystallized in complex with FKBP51 (Figure 6A). The 5-chloro-2-thienyl moiety is again located in the transient sub-pocket created by the crucial outward flip of Phe⁶⁷. The overlay with the SAFit1 cocrystal showed that both compounds bind nearly identical, the only substantial difference being the 5-chloro-2-thiophene vs the cyclohexyl moiety, with both moieties engaging in hydrophobic interactions with the protein (Figure 6B).

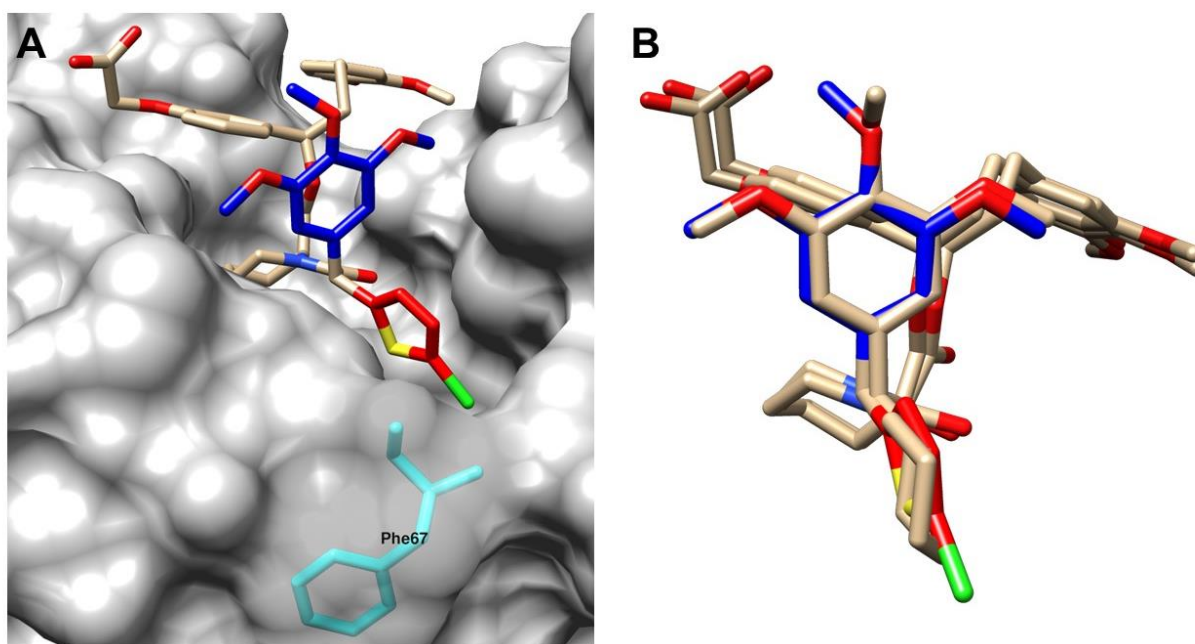
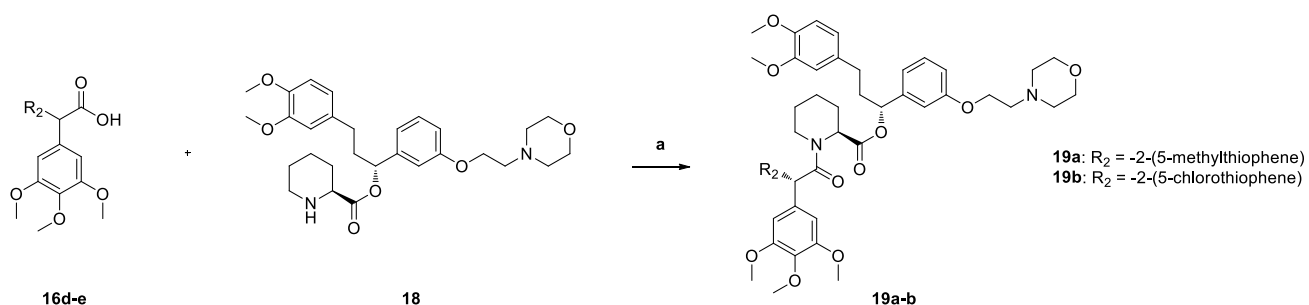


Figure 6: Co-crystal structure of compound **17e** (sticks) in complex with the FK1 domain of FKBP51 (grey surface, the displaced Phe⁶⁷ highlighted in cyan). The (5-chloro)thien-2-yl moiety is shown in red, the aryl moiety is shown in blue, and the rest of the ligand are shown in pale orange. (A) Co-crystal structure of compound **17e** in complex with the FK1 domain of FKBP51 (PDB: 8CCD). (B) Superposition of compound **17e** with SAFit1 (pale orange, from PDB: 8CCA).

Synthesis of thiophene-containing SAFit2 analogs

SAFit1 is the compound of choice for biochemical studies but it is poorly cell-permeable and lacks brain permeability. Its close analog SAFit2, however, has become the gold standard to pharmacologically interrogate FKBP51 *in vivo*. To explore, if this trend extended to the thiophene motif, we synthesized compounds **19a** and **19b** by amide coupling of the corresponding carboxylic acids **16d** and **16e** with the SAFit2 core/top group **18** (Scheme 4).

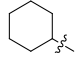
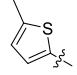
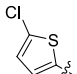
Scheme 4: Synthesis of the SAFit2 analogs **19a - b**.



Reagents and conditions: a) for **19a**: **16d**, **18**, TCFH, NMI, MeCN, rt; for **19b**: **16e**, **18**, oxalyl chloride, DIPEA, DCM, 0°C – rt.

After diastereomer separation, the active diastereomers of **19a** and **19b** were identified by affinity measurements, bound FKBP51 with high affinity. Moreover, these compounds were also tested in a nanoBRET assay³² to determine FKBP51 occupancy in intact cells (Table 3).

Table 3: Overview of the binding affinities, nano BRET data and determined *in-vivo* pharmacokinetic parameters of SAFit2 analogs **19a** and **19b**.

Entry	R ₂	FKBP51 K _i [nM]	FKBP52 K _i [nM]	Nano BRET FKBP51 IC ₅₀ [nM]	In-vivo pharmacokinetic parameters in BL6 mice			
					C _{max} [ng/mL]	t _{max} [h]	t _{1/2} [h]	V _D [L]
SAFit2		8 ± 1	2159 ± 175	196 ± 14	3061.0	1	3.7	0.1
19a		17 ± 3	775 ± 273	613 ± 58	-	-	-	-
19b		19 ± 3	774 ± 245	584 ± 41	989.8	0.5	4.3	0.3

Overall, compounds **19a** and **19b** had a similar profile to compared to SAFit2, albeit with a 3-fold offset in biochemical affinity as well as intracellular FKBP51 binding. This suggested the potential for *in vivo* studies. To explore this further, a preliminary PK study was performed in mice in direct comparison with SAFit2 (Table 3 and SI Table 2). This demonstrated an acceptable PK profile for **19b**, with a longer half-life time, higher volume of distribution and shorter t_{max} in the blood plasma than SAFit2. Furthermore, compound **19b** accumulated in gonadal white adipose tissue due to its high lipophilicity, and it also penetrated into the brain (SI Figure 4&5). This profile indicates that compound **19b** has sufficient *in vivo* stability and can pass the blood-brain barrier, suggesting its applicability as a tool compound to interrogate the function of FKBP51 in animal models.

Influence of the thiophene-containing SAFit analogs on TRPV1 desensitization

Knockout, knockdown, and pharmacological studies using SAFit2 have clearly established FKBP51 as an important factor in chronic pain states in mice.^{14,15,33,34} Recently, we showed that SAFit2 could desensitize the transient receptor potential cation channel subfamily V member 1 (TRPV1), which could contribute to the observed analgesic effects of SAFit2.¹⁶ Moreover, we showed that desensitization of TRPV1 channels occurred independent of FKBP51 inhibition. Since TRPV1 is a promising target for the treatment of chronic pain in itself, we explored if our novel SAFit2 analogs **19a** and **19b** could mimic the TRPV1-desensitizing effects of SAFit2. Therefore, we measured the effect on calcium influx of sensory neurons after stimulation with the TRPV1 agonist capsaicin before and after treatment with compounds **19a** and **19b** (Figure 7).

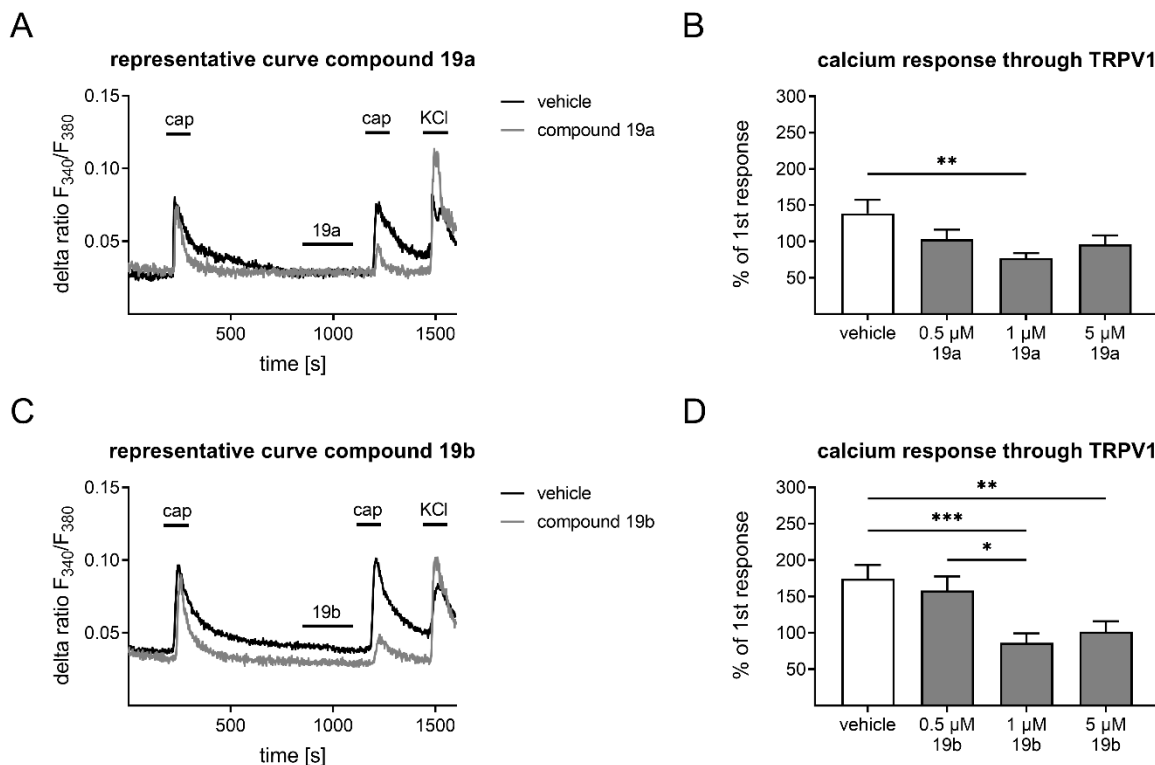


Figure 7: The influence of compounds **19a** and **19b** on TRPV1-mediated calcium influx in primary sensory neurons. (A, C) Representative graphs of TRPV1-mediated calcium responses from either vehicle or compound **19a** (A)/ compound **19b** (C) at a concentration of 1 μ M treated primary sensory neurons. (B, D) Quantification and comparison of TRPV1-mediated calcium responses before and after compound **19a** (B)/ compound **19b** (D) treatment. The quantification displays the mean \pm SEM from 25-42 measured primary sensory neurons per condition. * $p < 0.05$, ** $p < 0.01$, *** $p < 0.001$ was assessed with a one-way ANOVA with Tukey's multiple comparisons post hoc test. Abbreviations: cap: capsaicin, KCl: potassium chloride, TRPV1: transient receptor potential cation channel subfamily V member 1

Compounds **19a** and **19b** both showed about 50% reduction in calcium influx at a concentration of 1 μ M. Furthermore, compound **19a** seems slightly more potent at a lower concentration of 0.5 μ M.

Overall, the novel SAFit2 analogs **19a** and **19b** desensitize TRPV1 channel activity to almost the same extent as SAFit2. While the target underlying this effect is currently unknown, our results suggest that the cyclohexyl/thiophene moiety is not involved. Importantly, we previously showed

that the desensitization does not occur at the level of TRPV1 directly. Since direct inhibition of TRPV1 has been associated with undesired adverse effects, an indirect desensitization as effected by SAFit analogs might be more subtle way to manipulate TRPV1, which could exert analgesic effects via a dual mechanism (FKBP51 inhibition and TRPV1 desensitization).

CONCLUSION

Since the discovery of the first selective FKBP51 ligands SAFit1 and SAFit2, the cyclohexyl moiety has remained an indispensable structural motif for high affinity and selectivity over its closest homolog FKBP52. In this study, we serendipitously discovered 2-thienyl groups as functional cyclohexyl mimetics. We demonstrated that a methyl group in the C- α -position of the amide group is sufficient to induce selectivity over FKBP52. Structure-affinity relationship analysis revealed that the new motif is tolerant to substitutions in the 5-position of the thiophene group, resulting in cell-permeable compounds **19a** and **19b**, which maintained the TRPV1-desensitizing effect of SAFit2. The discovery of 5-substituted thiophenes open a new dimension in the structure-based design of selective FKBP51 inhibitors. Furthermore, compound **19b** qualifies as a novel tool compound for exploring the FKBP51 and in neuropathic pain states in mice.

EXPERIMENTAL SECTION

Primary sensory neuron cultures and calcium imaging

Primary sensory neuron cultures were prepared as previously described in Wedel et al., 2022.¹⁶ Briefly, dorsal root ganglia were collected from naïve mice with C57BL/NRj background. The tissue was enzymatically treated with collagenase, dispase and trypsin and afterwards mechanically dissociated, purified and primary sensory neurons were plated on poly-L-lysine

coated cover slips. The cells were incubated overnight at 37 °C and were used for calcium imaging experiments the next day. Calcium imaging was performed in a live cell imaging setup and a recently published protocol, which was used to determine the influence of SAFit2 on TRPV1.¹⁶ Briefly, primary sensory neurons were stained with Fura-2-AM for at least one hour. For measuring the total TRPV1-mediated calcium flux, stained sensory neurons were stimulated with the TRPV1 agonist capsaicin (100 nM, 20s) during live cell imaging. Afterwards, the agonist capsaicin was washed out and primary sensory neurons were incubated for two minutes with either the respective compounds or vehicle (DMSO), diluted in freshly prepared Ringer's solution, that contained that contained in 1445mM NaCl, 1.25mM CaCl₂, 1mM MgCl₂, 5mM KCl, 10mM D-glucose, and 10mM HEPES, adjusted to pH 7.3. In order to observe the influence of compound **19a** and **19b** on TRPV1, the cells were again stimulated with capsaicin (100 nM, 20s) immediately after the pretreatment phase with the respective compounds. At the end of each protocol, the cells were treated with potassium chloride (50 mM, 45s) to trigger depolarization and to identify reacting cells as primary sensory neurons.

Crystallization

Complexes were prepared by mixing FKBP51FK1 A19T, C103A, C107I (14-140) at 10-20 mg/ml with a slight molar excess of ligand previously dissolved at 20 mM in DMSO. Crystallization was performed at room temperature using the hanging drop vapor-diffusion method, equilibrating mixtures of 1 µl protein complex and 1 µl reservoir against 500 µl reservoir solution. Crystals were obtained from reservoir solutions containing 16-32% PEG-3350, 0.2 M NH₄-acetate, 0.1 M HEPES-NaOH pH 7.5 and for **4a** additionally 10% ethylene glycol. Crystals were fished, cryoprotected with 30% PEG-3350, 0.2 M NH₄-acetate, 0.1 M HEPES-NaOH pH 7.5 and 10% ethylene glycol and flash frozen in liquid nitrogen.

Structure solution and refinement

The crystallographic experiments were performed on the BL14.1 beamline at the Helmholtz-Zentrum BESSY II synchrotron, Berlin, Germany.³⁵ Diffraction data were integrated with DIALS or XDS and further processed with the implemented programs of the CCP4i and CCP4i2 interface.^{36–40} The data reduction was conducted with Aimless.^{39,41,42} Crystal structures were solved by molecular replacement using Phaser.⁴³ Iterative model improvement and refinement were performed with Coot and Refmac5.^{44–49} The dictionaries for the compounds were generated with PRODRG implemented in CCP4i.⁵⁰ Residues facing solvent channels without detectable side chain density were truncated.

General Information. Air and water-sensitive reactions were performed under argon atmosphere with commercially available dry solvents. All commercially available chemicals and solvents were used as received. Chromatographic separations were performed by manual flash chromatography on silica (SiO₂) from Macherey–Nagel (particle size 0.04–0.063 mm). Reverse-phase purifications were performed with a Interchim puriFlash 5.250 system fitted with a Luna® 5 µm C18(2) 100 Å, LC column (250 x 21.2 mm). Eluents were 0.1% TFA in water (eluent A) and 0.1% TFA in acetonitrile (eluent B). Thin-layer chromatography (TLC) was performed on precoated aluminum plates with a fluorescence indicator from Merck (silica gel 60 F254). ¹H NMR spectra, ¹³C NMR spectra, 2D HSQC, HMBC, COSY, and NOESY were obtained from the NMR Department of the Technical University of Darmstadt, on a Bruker DRX 500 spectrometer at room temperature, unless stated otherwise. Proton chemical shifts are expressed as parts per million (ppm, δ scale) and are referenced to residual solvent (¹H: CDCl₃, δ = 7.26; DMSO-d₆, δ = 2.50. ¹³C: CDCl₃, δ = 77.16; DMSO-d₆, δ = 39.52). Coupling constants (J) are given in hertz (Hz). Analytical LC–MS

(liquid chromatography–mass spectrometry) measurements were performed on an Agilent 1260 Infinity II System consisting of a 1260 Infinity II flexible pump, a vial sampler, a multicolumn thermostat, and a diode array detector connected to a 6125B MSD single quadrupole detector. Eluents were 0.1% formic acid in water (eluent A) and 0.1% formic acid in acetonitrile (eluent B). High-resolution mass spectra (HRMS) were obtained by the Mass Spectrometry Department of the Technical University of Darmstadt using a Bruker Daltonics Impact II mass spectrometer (quadrupole time-of-flight). Analytical HPLC analyses was performed on an Agilent 1260 Infinity II System consisting of a 1260 Infinity II flexible pump, a vialsampler, and a multicolumn thermostat fitted with a Poroshell 120 3 mm × 150 mm, 2.7 μm EC-C18 column or a Poroshell 120 50 mm × 2.1 mm, 1.9 μm EC-C18, a diode array detector, and a 6125B MSD single quadrupole detector (eluent A, 0.1% formic acid in water; eluent B, 0.1% formic acid in acetonitrile). Detailed measurement parameters (e.g., used gradient) were specified in the analytical data of the compounds. The purity of all tested compounds was ≥95% based on reverse phase HPLC ($\lambda = 220$ nm).

General Experimental Procedures.

General procedure A:

A 10 mL filter syringe was charged with resin **5** and the resin was swelled for 10 min in DCM. After filtration, the resin was washed with DMF and treated three times with a pre-cooled solution of 20 vol.-% 4-methylpiperidine in DMF for 5 min. After complete Fmoc deprotection, the resin was filtered and washed twice with DMF. Then a solution containing the respective carboxylic acid, HATU, HOAt, and DIPEA in DMF was added. The resulting suspension was shaken at rt overnight. Then the resin was filtered and washed twice with DMF, followed by DCM. Finally, the product was cleaved off the resin by treating it with a solution of 20 vol.-% HFIP in DCM for

1 h. After removal of the solvent under reduced pressure and purification via preparative HPLC, the respective compounds were obtained as white solids.

General procedure B.

A 10 mL filter syringe was charged with resin **5**, and the resin was swelled for 10 min in DCM. After filtration, the resin was washed with DMF and treated three times with a pre-cooled solution of 20 vol.-% 4-methylpiperidine in DMF for 5 min. After complete Fmoc deprotection, the resin was filtered and washed twice with DMF, followed by DCM. In a flask, the respective carboxylic acid was dissolved in DCM. Then PPh₃ was added, followed by trichloroacetonitrile. The resulting solution was stirred for 1h at rt. After the complete formation of the acid chloride, the Fmoc deprotected resin was treated first with a solution of DIPEA in DCM, followed by the acid chloride solution. The resulting suspension was shaken for 1h at rt. Then the resin was filtered and washed twice with DCM. Finally, the product was cleaved off the resin by treating it with a solution of 20 vol.-% HFIP in DCM for 1 h. After removal of the solvent under reduced pressure and purification via preparative HPLC, the respective compounds were obtained as white solids.

General procedure C.

A 10 mL filter syringe was charged with resin **5**, and the resin was swelled for 10 min in DCM. After filtration, the resin was washed with DMF and treated three times with a pre-cooled solution of 20 vol.-% 4-methylpiperidine in DMF for 5 min. After complete Fmoc deprotection, the resin was filtered and washed twice with DMF, followed by DCM. In a flask, the respective carboxylic acid was dissolved in DCM and cooled to 0°C. Then oxalyl chloride was added, and the resulting solution was stirred at rt for 1h. After the complete formation of the acid chloride, the solvent was removed under reduced pressure, and the obtained acid chloride was redissolved in DCM. The

Fmoc deprotected resin was treated first with a solution of DIPEA in DCM, followed by the addition of the acid chloride solution. The resulting suspension was shaken for 1h at rt. Then the resin was filtered and washed twice with DCM. Finally, the product was cleaved off the resin by treating it with a solution of 20 vol.-% HFIP in DCM for 1 h. After removal of the solvent under reduced pressure and purification via preparative HPLC, the respective compounds were obtained as white solids.

(2R,5S,12S)-12-(2-thienyl)-2-[2-(3,4-dimethoxyphenyl)ethyl]-15,15-dimethyl-3,19-dioxo-10,13,16-triazatricyclo[18.3.1.0^{5,10}]tetracos-1(24),20,22-triene-4,11,14,17-tetrone ((S)-9)

A 10 mL filter syringe was charged with resin **5** (180 mg, 0.10 mmol, 1.00 eq., loading: 0.56 mmol/g), and the resin was swelled for 10 min in DCM. After filtration, the resin was washed with DMF and treated three times with a solution of 20 vol.-% 4-methylpiperidine in DMF for 5 min. After complete Fmoc deprotection, the resin was filtered and washed twice with DMF. The obtained resin was then treated with a solution containing Fmoc-2-thienylglycine (**6**, 117 mg, 0.31mmol, 3.00 eq.), HATU (117 mg, 0.31 mmol, 3.00 eq.), HOAt (42 mg, 0.31 mmol, 3.00 eq.) and DIPEA (106 μ L, 0.61 mmol, 6.00 eq.) in 1mL DMF for 2 h at rt. Next, the resin was filtered and washed three times with DMF, followed by THF (3x) and DCM (3x). Then the Fmoc protection group was removed by treating resin **7** with a pre-cooled solution of 20 vol.-% 4-methylpiperidine in DMF for 5 min (0°C), filtering, and washing with DMF. This step was repeated three times to ensure full Fmoc deprotection. Afterward, the obtained resin was treated with a solution of Fmoc-Aib-OH (66 mg, 0.20 mmol, 1.95 eq.), HATU (77 mg, 0.20 mmol, 1.95 eq.), and DIPEA (70 μ L, 0.40 mmol, 3.90 eq.) in 1 mL DMF at rt under shaking overnight. The resin was then washed with DMF three times, and the Fmoc protection group was removed as previously described by the treatment with a pre-cooled solution of 20 vol.-% 4-methylpiperidine

in DMF. Next, the resin was washed with DMF, followed by DCM, and the product was cleaved of the resin by treating it with a 20 vol.-% solution of HFIP in DCM for 1 h. After filtration of the resin, the solution was concentrated under reduced pressure and was dissolved in 10 mL DMF. Then HATU (117 mg, 0.31 mmol, 3.00 eq.) was added, followed by DIPEA (88 μ L, 0.51 mmol, 5.00 eq.), and the resulting solution was stirred at rt overnight. After the complete macrocyclization, the solvent was removed, and the crude was purified by preparative HPLC (5 - 100%, solvent B). The diastereomer (**S**)-**9** (7 mg, 10.54 μ mol, 11%) was obtained as a solid after the removal of the solvent. HPLC (5 - 100 % solvent B, 3 min) R_t = 2.125min, purity (220 nm): 99%. HRMS (ESI⁺): m/z: calculated 664.26802 [M+H]⁺, found 664.26878 [M+H]⁺. ¹H NMR (500 MHz, Chloroform-d) δ 7.25 – 7.18 (m, 1H), 7.05 – 7.00 (m, 2H), 6.98 – 6.93 (m, 2H), 6.90 (dd, J = 5.1, 3.6 Hz, 1H), 6.84 (dd, J = 8.3, 2.6 Hz, 1H), 6.79 (dd, J = 7.9, 2.5 Hz, 1H), 6.72 – 6.68 (m, 2H), 5.86 (d, J = 7.3 Hz, 1H), 5.79 (dd, J = 9.0, 4.3 Hz, 1H), 4.60 (d, J = 2.6 Hz, 1H), 4.54 (d, J = 7.5 Hz, 1H), 4.09 (dd, J = 8.8, 4.6 Hz, 1H), 3.88 (s, 3H), 3.86 (s, 3H), 3.55 – 3.46 (m, 1H), 3.24 – 3.12 (m, 1H), 2.67 – 2.53 (m, 2H), 2.41 – 2.30 (m, 1H), 2.29 – 2.20 (m, 1H), 2.13 – 2.07 (m, 2H), 1.97 – 1.90 (m, 2H), 1.85 – 1.76 (m, 2H), 1.74 – 1.69 (m, 1H), 1.66 – 1.60 (m, 1H), 1.57 (s, 3H), 1.51 (s, 3H).

2-(3-(((1R)-1-(((2S)-1-(2-Cyclohexyl-2-(thiophen-2-yl)acetyl)piperidine-2-carbonyloxy)-3-(3,4-dimethoxyphenyl)propyl)phenoxy)acetic acid (4a)

Following the general procedure A compound **4a** was synthesized using resin **5** (107 mg, 0.08 mmol, 1.00 eq, loading: 0.73 mmol/g), **I** (35 mg, 0.16 mmol, 2.00 eq.), HATU (59 mg, 0.16 mmol, 2.00 eq.), HOAt (21 mg, 0.16 mmol, 2.00 eq.) DIPEA (70 μ L, 0.39 mmol, 5.00 eq.) and 1.60 mL DMF. After purification via preparative HPLC (50 - 100%, solvent B), compound **4a** (28 mg, 42.18 μ mol, 54%) was obtained as a white solid. HPLC (50 – 100 % solvent B, 3 min) R_t = 1.737 min, purity (220 nm): 97%. HRMS (ESI⁺): m/z: 664.29386 calculated [M+H]⁺, found 664.29417 [M+H]⁺. ¹H NMR (500 MHz, CDCl₃) δ 7.26 – 7.21 (m, 1H), 7.19 – 7.15 (m, 1H), 6.93 – 6.90 (m,

1H), 6.89 – 6.86 (m, 2H), 6.84 – 6.81 (m, 1H), 6.80 – 6.76 (m, 1H), 6.71 – 6.64 (m, 3H), 5.73 – 5.59 (m, 1H), 5.54 – 5.48 (m, 1H), 4.72 – 4.58 (m, 2H), 4.07 – 3.99 (m, 1H), 3.86 (s, 3H), 3.85 (s, 3H), 3.40 – 2.95 (m, 1H), 2.70 – 2.51 (m, 2H), 2.35 – 2.18 (m, 2H), 2.10 – 1.99 (m, 2H), 1.91 – 1.75 (m, 1H), 1.71 – 1.49 (m, 5H), 1.49 – 1.32 (m, 3H), 1.20 – 1.03 (m, 4H), 0.92 – 0.66 (m, 3H). ¹³C NMR (125 MHz, CDCl₃) δ 173.32, 172.56, 171.69, 171.49, 170.54, 170.25, 158.08, 157.81, 149.04, 148.96, 147.53, 147.43, 142.23, 142.20, 141.06, 140.36, 133.67, 133.53, 129.83, 129.80, 126.50, 126.47, 125.95, 125.75, 124.81, 124.78, 120.38, 120.32, 119.94, 119.82, 115.53, 115.06, 111.96, 111.83, 111.55, 111.48, 111.42, 110.69, 76.45, 76.12, 65.47, 65.37, 56.07, 56.02, 52.75, 52.58, 49.72, 49.66, 44.14, 44.11, 42.69, 42.58, 38.23, 37.99, 32.43, 32.24, 31.56, 31.37, 30.69, 29.84, 27.14, 26.84, 26.53, 26.50, 26.15, 26.06, 25.65, 25.22, 21.12, 21.03.

2-(3-((R)-1-(((S)-1-(2-(5-Chlorothiophen-2-yl)-2-cyclohexylacetyl)piperidine-2-carbonyl)-oxy)-3-(3,4-dimethoxyphenyl)propyl)phenoxy)acetic acid (4b)

Following the general procedure A compound **4b** was synthesized using: Resin **5** (99 mg, 0.04 mmol, 1.00 eq, loading: 0.39 mmol/g), **II** (20 mg, 0.08 mmol, 2.00 eq.), HATU (29 mg, 0.08 mmol, 2.00 eq.), HOAt (11 mg, 0.08 mmol, 2.00 eq.) DIPEA (34 μL, 0.19 mmol, 5.00 eq.) and 1.00 mL DMF. After purification via column chromatography (CH/EtOAc + 1% FA, 2:1), compound **4b** (18 mg, 25.78 μmol, 99%) was obtained as a white solid. HPLC (50 – 100 % solvent B, 3 min) R_t = 1.563 min, purity (220 nm): 95%. HRMS (ESI⁺): m/z: 698.2552 calculated [M+H]⁺, found 698.2552 [M+H]⁺. ¹H NMR (500 MHz, CDCl₃) δ 7.26 – 7.17 (m, 1H), 6.93 – 6.86 (m, 1H), 6.85 – 6.82 (m, 1H), 6.78 (t, J = 3.9 Hz, 1H), 6.74 – 6.70 (m, 1H), 6.69 – 6.67 (m, 1H), 6.65 (s, 1H), 6.64 – 6.60 (m, 1H), 5.72 – 5.62 (m, 1H), 5.49 (t, J = 7.5 Hz, 1H), 4.71 – 4.62 (m, 2H), 4.00 – 3.91 (m, 1H), 3.86 (s, 3H), 3.85 (s, 3H), 3.81 – 3.74 (m, 1H), 3.32 (td, J = 13.1, 3.0 Hz, 1H), 2.68 – 2.60 (m, 1H), 2.60 – 2.52 (m, 1H), 2.37 – 2.26 (m, 1H), 2.25 – 2.17 (m, 1H), 2.12 – 2.02 (m, 1H), 2.00 – 1.90 (m, 0H), 1.82 – 1.72 (m, 1H), 1.71 – 1.57 (m, 6H), 1.54 – 1.41 (m, 2H), 1.37 – 1.21 (m, 4H), 1.20 – 1.06 (m, 2H), 0.96 – 0.73 (m, 2H). ¹³C NMR (125 MHz, CDCl₃) δ 172.82, 172.05, 171.54, 171.35, 170.28, 170.02, 157.94, 157.71, 148.95, 148.88, 147.44, 147.35, 142.03, 141.99, 139.90, 139.19, 133.39, 129.71, 125.24, 125.18, 125.03, 124.98, 120.26, 120.21, 119.82, 119.74, 115.34, 114.87, 111.85, 111.77, 111.42, 111.39, 110.77, 76.37, 76.12, 65.32, 55.96, 55.90, 52.68, 52.51, 50.18, 44.11, 44.07, 42.83, 42.56, 38.05, 37.84, 32.12, 31.84, 31.40, 31.22, 30.49, 26.96, 26.71, 26.29, 26.27, 25.97, 25.89, 25.50, 25.23, 20.92, 20.88.

2-(3-((R)-1-(((S)-1-((S)-2-(5-Chlorothiophen-2-yl)pent-4-enoyl)piperidine-2-carbonyl)oxy)-3-(3,4-dimethoxyphenyl)propyl)phenoxy)acetic acid ((S)-13a)

Following the general procedure A compound (**S**)-**13a** was synthesized using: Resin **5** (201 mg, 0.08 mmol, 1.00 eq, loading: 0.39 mmol/g), **12a** (34 mg, 0.16 mmol, 2.00 eq.), HATU (60 mg, 0.16 mmol, 2.00 eq.), HOAt (21 mg, 0.16 mmol, 2.00 eq.) DIPEA (68 μ L, 0.39 mmol, 5.00 eq.) and 1.57 mL DMF. After purification via preparative HPLC (50 - 80%, solvent B) (**S**)-**13a** (20 mg, 30.48 μ mol, 39%) was obtained as a white solid. HPLC (50 – 100 % solvent B, 3 min) R_t = 1.606 min, purity (220 nm): 99%. HRMS (ESI⁺): m/z: calculated 656.20794 [M+H]⁺, found 656.20771 [M+H]⁺. ¹H NMR (500 MHz, CDCl₃) δ 7.31 – 7.27 (m, 2H), 6.91 (dt, J = 7.7, 2.2 Hz, 2H), 6.83 – 6.78 (m, 2H), 6.75 (d, J = 3.7 Hz, 1H), 6.72 (d, J = 1.9 Hz, 1H), 6.70 (t, J = 2.9 Hz, 1H), 6.67 (d, J = 3.8 Hz, 1H), 5.67 (ddd, J = 17.2, 9.3, 3.9 Hz, 2H), 5.50 (d, J = 5.5 Hz, 1H), 5.05 – 4.93 (m, 2H), 4.76 – 4.62 (m, 2H), 4.07 (t, J = 7.3 Hz, 1H), 3.89 (s, 3H), 3.88 (s, 3H), 3.39 (td, J = 13.2, 3.0 Hz, 1H), 2.80 – 2.65 (m, 2H), 2.66 – 2.55 (m, 1H), 2.53 – 2.44 (m, 1H), 2.35 (d, J = 13.8 Hz, 1H), 2.31 – 2.20 (m, 1H), 2.16 – 1.97 (m, 1H), 1.78 – 1.67 (m, 2H), 1.63 (d, J = 13.6 Hz, 1H), 1.45 – 1.29 (m, 1H), 1.24 – 1.11 (m, 1H). ¹³C NMR (126 MHz, CDCl₃) δ 172.21, 171.30, 170.22, 158.13, 149.09, 147.59, 142.24, 140.36, 134.77, 133.45, 129.90, 129.28, 125.57, 124.81, 120.33, 119.73, 117.81, 115.94, 111.82, 111.51, 109.93, 65.52, 56.09, 56.05, 52.92, 44.29, 43.92, 39.51, 38.25, 31.64, 27.02, 25.14, 21.00.

2-(3-((R)-1-(((S)-1-((S)-2-(5-Chlorothiophen-2-yl)butanoyl)piperidine-2-carbonyl)-oxy)-3-(3,4-dimethoxyphenyl)propyl)phenoxy)acetic acid ((S)-13b)

Following the general procedure A compound (**S**)-**13b** was synthesized using: Resin **5** (129 mg, 0.07 mmol, 1.00 eq, loading: 0.56 mmol/g), **12b** (30 mg, 0.15 mmol, 2.00 eq.), HATU (56 mg, 0.15 mmol, 2.00 eq.), HOAt (20 mg, 0.15 mmol, 2.00 eq.), DIPEA (64 μ L, 0.37 mmol, 5.00 eq.) and 1.47 mL DMF. After purification via preparative HPLC (50 - 80%, solvent B), compound (**S**)-**13b** (10 mg, 15.06 μ mol, 21%) was obtained as a white solid. HPLC (50 – 100 % solvent B, 3 min) R_t = 1.600 min, purity (220 nm): 99%. HRMS (ESI⁺): m/z: calculated 644.20794 [M+H]⁺, found 644.20792 [M+H]⁺. ¹H NMR (500 MHz, CDCl₃) δ 7.23 (s, 1H), 6.87 (d, J = 7.7 Hz, 1H), 6.85 – 6.82 (m, 1H), 6.79 (d, J = 8.1 Hz, 1H), 6.77 (s, 1H), 6.74 (d, J = 3.7 Hz, 1H), 6.71 – 6.65 (m, 3H), 5.66 (dd, J = 8.8, 5.0 Hz, 1H), 5.52 – 5.44 (m, 1H), 4.76 – 4.61 (m, 2H), 3.92 – 3.88 (m, 1H), 3.87 (s, 3H), 3.86 (s, 3H), 3.41 – 3.31 (m, 1H), 2.71 – 2.65 (m, 1H), 2.63 – 2.54 (m, 1H), 2.35

(d, $J = 14.3$ Hz, 1H), 2.27 – 2.19 (m, 1H), 2.10 – 2.04 (m, 1H), 1.98 – 1.90 (m, 1H), 1.82 – 1.55 (m, 5H), 1.40 – 1.29 (m, 1H), 1.23 – 1.11 (m, 1H), 0.79 (t, $J = 7.4$ Hz, 3H). ^{13}C NMR (126 MHz, CDCl_3) δ 172.93, 170.14, 158.21, 149.09, 147.58, 142.23, 140.79, 133.46, 129.85, 129.01, 125.63, 124.74, 120.33, 119.70, 116.13, 111.81, 111.51, 109.73, 76.81, 65.60, 56.09, 56.04, 53.04, 45.83, 43.99, 38.27, 31.67, 28.61, 26.94, 25.17, 21.07, 11.97.

2-(3-((R)-1-(((S)-1-((S)-2-(5-Chlorothiophen-2-yl)propanoyl)piperidine-2-carbonyloxy)-3-(3,4-dimethoxyphenyl)propyl)phenoxy)acetic acid ((S)-13c)

Following the general procedure A compound **(S)-13c** was synthesized using: Resin **5** (282 mg, 0.11 mmol, 1.00 eq, loading: 0.56 mmol/g), **12c** (21 mg, 0.11 mmol, 1.00 eq.), HATU (42 mg, 0.11 mmol, 1.00 eq.), HOAt (15 mg, 0.11 mmol, 1.00 eq.), DIPEA (48 μL , 0.28 mmol, 2.50 eq.) and 1.10 mL DMF. After purification via preparative HPLC (70 - 100%, solvent B), compound **(S)-13c** (14 mg, 22.21 μmol , 20%) was obtained as a white solid. HPLC (50 – 100 % solvent B, 3 min) $R_t = 2.239$ min, purity (220 nm): 98%. HRMS (ESI⁺): m/z : calculated 630.1923 [M+H]⁺, found 630.1924 [M+H]⁺. ^1H NMR (500 MHz, CDCl_3) δ 7.25 – 7.21 (m, 1H), 6.92 – 6.85 (m, 2H), 6.82 – 6.77 (m, 2H), 6.75 – 6.68 (m, 3H), 6.64 (d, $J = 3.8$ Hz, 1H), 5.65 (dd, $J = 8.8, 4.9$ Hz, 1H), 5.53 – 5.42 (m, 1H), 4.73 – 4.59 (m, 2H), 3.87 (s, 3H), 3.86 (s, 3H), 3.85 – 3.84 (m, 1H), 3.39 (td, $J = 13.2, 3.1$ Hz, 1H), 2.70 – 2.64 (m, 1H), 2.62 – 2.56 (m, 1H), 2.38 – 2.30 (m, 1H), 2.28 – 2.19 (m, 1H), 2.11 – 2.02 (m, 1H), 1.76 – 1.66 (m, 2H), 1.62 (d, $J = 13.8$ Hz, 1H), 1.43 (d, $J = 6.8$ Hz, 3H), 1.39 – 1.30 (m, 1H), 1.26 – 1.15 (m, 1H). ^{13}C NMR (126 MHz, CDCl_3) δ 173.27, 171.36, 170.31, 158.22, 149.16, 147.66, 142.79, 142.30, 133.50, 129.92, 128.89, 125.68, 123.94, 120.38, 119.69, 116.15, 111.92, 111.61, 109.79, 76.90, 65.65, 56.12, 52.97, 43.85, 38.65, 38.24, 31.66, 27.09, 25.11, 20.99.

2-(3-((R)-3-(3,4-Dimethoxyphenyl)-1-(((S)-1-((S)-2-(thiophen-2-yl)-2-(3,4,5-tri-methoxy-phenyl)acetyl)piperidine-2-carbonyloxy)propyl)phenoxy)acetic acid (17a)

Following the general procedure B compound **17a** was synthesized using: Resin **5** (200 mg, 0.08 mmol, 1.00 eq, loading: 0.39 mmol/g), **16a** (24 mg, 0.08 mmol, 1.00 eq.), PPh_3 (41 mg, 0.16 mmol, 2.00 eq.), trichloroacetonitrile (16 μL , 0.16 mmol, 2.00 eq.), DIPEA (68 μL , 0.39 mmol, 5.00 eq.) and 1 mL DCM. After purification via preparative HPLC (50 - 70%, solvent B), compound **17a**

(10 mg, 13.37 μmol , 17%) was obtained as a white solid. HPLC (70 – 100 % solvent B, 3 min) R_t = 2.145 min, purity (220 nm): 99%. HRMS (ESI⁺): m/z : calculated 748.2786 [M+H]⁺, found 748.2788 [M+H]⁺. ¹H NMR (500 MHz, CDCl₃) δ 7.16 – 7.14 (m, 1H), 7.13 (d, J = 7.8 Hz, 1H), 6.84 (dd, J = 5.1, 3.5 Hz, 1H), 6.80 – 6.75 (m, 2H), 6.74 – 6.69 (m, 2H), 6.66 – 6.65 (m, 1H), 6.62 – 6.58 (m, 2H), 6.26 (s, 2H), 5.45 (dd, J = 9.0, 4.7 Hz, 1H), 5.41 – 5.39 (m, 1H), 5.32 (s, 1H), 4.71 – 4.45 (m, 2H), 3.78 (s, 3H), 3.77 (s, 3H), 3.76 – 3.74 (m, 1H), 3.70 (s, 3H), 3.46 (s, 6H), 3.08 (td, J = 13.3, 3.2 Hz, 1H), 2.66 – 2.56 (m, 1H), 2.54 – 2.44 (m, 1H), 2.29 – 2.22 (m, 1H), 2.18 – 2.08 (m, 1H), 1.99 – 1.90 (m, 1H), 1.80 – 1.67 (m, 2H), 1.63 – 1.56 (m, 1H), 1.42 – 1.31 (m, 1H), 1.31 – 1.19 (m, 1H). ¹³C NMR (126 MHz, CDCl₃) δ 172.03, 170.80, 170.39, 158.30, 153.47, 149.18, 147.65, 142.68, 142.37, 137.15, 133.64, 133.46, 129.70, 126.65, 126.36, 125.92, 120.38, 119.52, 116.06, 111.88, 111.59, 108.82, 105.37, 77.05, 65.53, 60.92, 56.11, 56.07, 56.02, 52.92, 50.28, 44.18, 38.59, 31.72, 27.23, 25.20, 20.75.

2-(3-((R)-3-(3,4-Dimethoxyphenyl)-1-(((S)-1-((S)-2-phenyl-2-(3,4,5-trimethoxy-phenyl)-acetyl)piperidine-2-carbonyloxy)propyl)phenoxy)acetic acid (17b)

A 10 mL filter syringe was charged with resin **5** (150 mg, 0.10 mmol, 1.00 eq., loading: 0.45 mmol/g), and the resin was swelled for 10 min in DCM. After filtration, the resin was washed with DMF and treated three times with a pre-cooled solution of 20 vol.-% 4-methylpiperidine in DMF for 5 min. After complete Fmoc deprotection, the resin was filtered and washed twice with DMF. The resin was then treated with a solution of **16b** (31 mg, 0.07 mmol, 1.50 eq.), COMU (43 mg, 0.10 mmol, 1.50 eq.), pyridine (16 μL , 0.20 mmol, 3.00 eq.) in 0.68 mL DMF. The reaction mixture was then stirred at rt overnight. After complete conversion, the resin was filtered and washed twice with 3 mL DMF and 3 mL DCM. Finally, the product was cleaved off the resin by treating it with a solution of 20 vol.-% HFIP in DCM for 1 h. After purification via preparative HPLC (50 – 70%, solvent B) compound **17b** (17 mg, 22.92 μmol , 34%) was obtained as a white solid. HPLC (50 – 100 % solvent B, 3 min) R_t = 1.399 min, purity (220 nm): 96%. HRMS (ESI⁺): m/z : calculated 742.32219 [M+H]⁺, found 742.32158 [M+H]⁺. ¹H NMR (500 MHz, CDCl₃) δ 7.37 – 7.27 (m, 5H), 7.21 (d, J = 7.5 Hz, 2H), 6.94 – 6.90 (m, 1H), 6.86 (dd, J = 16.3, 7.7 Hz, 2H), 6.81 – 6.79 (m, 1H), 6.74 (d, J = 9.9 Hz, 2H), 6.33 (s, 2H), 5.59 (dd, J = 9.1, 4.7 Hz, 1H), 5.54 (d, J = 5.9 Hz, 1H), 5.21 (s, 1H), 4.67 (q, J = 16.2 Hz, 2H), 3.91 (s, 3H), 3.91 (s, 3H), 3.84 (s, 3H), 3.59

(s, 6H), 3.26 (t, $J = 11.7$ Hz, 1H), 2.79 – 2.71 (m, 1H), 2.68 – 2.59 (m, 1H), 2.43 – 2.34 (m, 1H), 2.31 – 2.23 (m, 1H), 2.12 – 2.04 (m, 1H), 1.89 – 1.77 (m, 2H), 1.70 (d, $J = 10.4$ Hz, 1H), 1.47 – 1.36 (m, 2H). ^{13}C NMR (126 MHz, CDCl_3) δ 173.09, 171.09, 170.49, 158.24, 153.33, 149.09, 147.57, 142.69, 139.33, 136.74, 133.65, 133.42, 129.69, 129.48, 128.49, 127.35, 120.34, 119.45, 116.02, 111.77, 111.49, 108.75, 105.87, 77.07, 65.41, 60.90, 56.07, 56.03, 55.92, 55.43, 52.80, 44.09, 38.59, 31.71, 27.31, 25.18, 20.78.

2-(3-((R)-3-(3,4-Dimethoxyphenyl)-1-((S)-1-((R)-2-(thiophen-3-yl)-2-(3,4,5-trimethoxyphenyl)acetyl)piperidine-2-carbonyloxy)propyl)phenoxy)acetic acid (17c)

A 10 mL filter syringe was charged with resin **5** (150 mg, 0.07 mmol, 1.00 eq., loading: 0.45 mmol/g), and the resin was swelled for 10 min in DCM. After filtration, the resin was washed with DMF and treated three times with a pre-cooled solution of 20 vol.-% 4-methylpiperidine in DMF for 5 min. After complete Fmoc deprotection, the resin was filtered and washed twice with DMF. The obtained resin was then treated with a solution containing **16c** (29 mg, 0.08 mmol, 1.00 eq.), T3P (80 μL , 0.14 mmol, 2.00 eq.), and pyridine (16 μL , 0.20 mmol, 3.00 eq.) in 0.68 mL DMF overnight. After the complete conversion of the starting material, the resin was filtered and washed twice with DMF, followed by DCM. Finally, the product was cleaved off the resin by treating it with a solution of 20 vol.-% HFIP in DCM for 1 h. After removal of the solvent under reduced pressure and purification via preparative HPLC. The respective compounds were obtained as white solids. After purification via preparative HPLC (50 - 70%, solvent B), compound **17c** (8 mg, 10.69 μmol , 16%) was obtained as a white solid. HPLC (30 – 100 % solvent B, 3 min) $R_t = 1.818$ min, purity (220 nm): 99%. HRMS (ESI⁺): m/z : calculated 748.27861 $[\text{M}+\text{H}]^+$, found 748.27844 $[\text{M}+\text{H}]^+$. ^1H NMR (500 MHz, CDCl_3) δ 7.28 (s, 1H), 7.26 – 7.21 (m, 1H), 7.03 – 6.96 (m, 2H), 6.93 – 6.87 (m, 1H), 6.82 (t, $J = 7.9$ Hz, 2H), 6.77 – 6.74 (m, 1H), 6.71 (d, $J = 8.8$ Hz, 2H), 6.31 (s, 2H), 5.53 (dt, $J = 15.6, 5.2$ Hz, 2H), 5.24 (s, 1H), 4.71 – 4.58 (m, 2H), 3.88 (s, 3H), 3.88 (s, 3H), 3.86 – 3.84 (m, 1H), 3.80 (s, 3H), 3.55 (s, 6H), 3.19 (td, $J = 13.1, 3.0$ Hz, 1H), 2.76 – 2.67 (m, 1H), 2.65 – 2.54 (m, 1H), 2.35 (d, $J = 14.1$ Hz, 1H), 2.29 – 2.16 (m, 1H), 2.08 – 2.01 (m, 1H), 1.87 – 1.72 (m, 2H), 1.72 – 1.60 (m, 1H), 1.49 – 1.32 (m, 2H). ^{13}C NMR (126 MHz, CDCl_3) δ 172.74, 170.84, 170.44, 158.28, 153.41, 149.12, 147.59, 142.74, 139.92, 136.82, 133.50, 133.41, 129.68, 128.81, 125.67, 123.09, 120.35, 119.44, 116.20, 111.77, 111.49, 108.45, 65.49, 60.91, 56.09, 56.04, 55.95, 52.76, 50.80, 44.12, 38.64, 31.75, 27.33, 25.21, 20.74.

2-(3-((R)-3-(3,4-Dimethoxyphenyl)-1-(((S)-1-((S)-2-(5-methylthiophen-2-yl)-2-(3,4,5-trimethoxyphenyl)acetyl)piperidine-2-carbonyl)oxy)propyl)phenoxy)-acetic acid (17d)

Following the general procedure B compound **17d** was synthesized using: Resin **5** (82 mg, 0.05 mmol, 1.00 eq., loading: 0.56 mmol/g), **16d** (30 mg, 0.09 mmol, 2.00 eq.), PPh₃ (49 mg, 0.19 mmol, 4.00 eq.), trichloroacetonitrile (19 μL, 0.19 mmol, 4.00 eq.), DIPEA (81 μL, 0.47 mmol, 10.00 eq.) and 0.93 mL DCM. After purification via preparative HPLC (50 - 80%, solvent B), compound **17d** (12 mg, 15.75 μmol, 34%) was obtained as a white solid. HPLC (50 - 100 % solvent B, 3 min) R_t = 1.484 min, purity (220 nm): 95%. HRMS (ESI⁺): m/z: calculated 762.29426 [M+H]⁺, found 762.29421 [M+H]⁺. ¹H NMR (500 MHz, CDCl₃) δ 7.24 (t, J = 7.9 Hz, 1H), 6.90 - 6.86 (m, 1H), 6.84 - 6.80 (m, 2H), 6.76 (d, J = 2.6 Hz, 1H), 6.71 (d, J = 9.1 Hz, 2H), 6.64 (d, J = 3.4 Hz, 1H), 6.57 (d, J = 3.4 Hz, 1H), 6.36 (s, 2H), 5.56 (dd, J = 9.0, 4.7 Hz, 1H), 5.51 (d, J = 5.9 Hz, 1H), 5.33 (s, 1H), 4.73 - 4.59 (m, 2H), 3.89 (s, 3H), 3.88 (s, 3H), 3.89 - 3.81 (m, 1H), 3.80 (s, 3H), 3.57 (s, 6H), 3.17 (td, J = 13.3, 3.0 Hz, 1H), 2.75 - 2.66 (m, 1H), 2.63 - 2.56 (m, 1H), 2.43 (s, 3H), 2.40 - 2.33 (m, 1H), 2.25 - 2.18 (m, 1H), 2.10 - 2.03 (m, 1H), 1.87 - 1.75 (m, 2H), 1.70 - 1.65 (m, 1H), 1.51 - 1.41 (m, 1H), 1.40 - 1.29 (m, 1H). ¹³C NMR (126 MHz, CDCl₃) δ 172.05, 170.94, 170.24, 158.08, 153.25, 148.96, 147.44, 142.51, 140.39, 139.60, 136.83, 133.62, 133.29, 129.57, 126.24, 124.23, 120.22, 119.37, 115.75, 111.65, 111.36, 108.84, 105.12, 76.85, 65.35, 60.78, 55.95, 55.90, 55.85, 52.76, 50.35, 44.01, 38.42, 31.57, 27.08, 25.06, 20.64, 15.35.

2-(3-((R)-1-(((S)-1-((S)-2-(5-Chlorothiophen-2-yl)-2-(3,4,5-trimethoxyphenyl)-acetyl)-piperidine-2-carbonyl)oxy)-3-(3,4-dimethoxyphenyl)propyl)phenoxy)-acetic acid (17e)

Following the general procedure B compound **17e** was synthesized using: Resin **5** (77 mg, 0.04 mmol, 1.00 eq., loading: 0.56 mmol/g), **16e** (15 mg, 0.04 mmol, 1.00 eq.), PPh₃ (23 mg, 0.09 mmol, 2.00 eq.), trichloroacetonitrile (9 μL, 0.09 mmol, 2.00 eq.), DIPEA (38 μL, 0.22 mmol, 5.00 eq.) and 0.5 mL DCM. After purification via preparative HPLC (50 - 70%, solvent B), compound **17e** (8 mg, 10.23 μmol, 24%) was obtained as a white solid. HPLC (50 - 100 % solvent B, 3 min) R_t = 2.253 min, purity (220 nm): 99%. HRMS (ESI⁺): m/z: calculated 782.2396 [M+H]⁺, found 782.2403 [M+H]⁺. ¹H NMR (500 MHz, CDCl₃) δ 7.21 (t, J = 7.8 Hz, 1H), 6.89 - 6.83 (m, 1H), 6.80 - 6.75 (m, 2H), 6.73 (s, 1H), 6.70 (dd, J = 5.4, 2.8 Hz, 2H), 6.67 (s, 1H), 6.62 (d, J = 3.8 Hz, 1H), 6.31 (s, 2H), 5.52 (dd, J = 9.0, 4.7 Hz, 1H), 5.47 (d, J = 6.6 Hz, 1H), 5.27 (s, 1H), 4.72 - 4.57 (m, 2H), 3.86 (s, 3H), 3.85 (s, 3H), 3.78 (s, 3H), 3.77 - 3.70 (m, 1H), 3.54 (s, 6H), 3.14 -

3.06 (m, 1H), 2.73 – 2.64 (m, 1H), 2.61 – 2.52 (m, 1H), 2.37 – 2.30 (m, 1H), 2.24 – 2.16 (m, 1H), 2.06 – 1.97 (m, 1H), 1.87 – 1.74 (m, 1H), 1.68 (d, J = 13.4 Hz, 1H), 1.52 – 1.42 (m, 1H), 1.37 – 1.23 (m, 2H). ¹³C NMR (126 MHz, CDCl₃) δ 171.22, 170.05, 169.26, 158.08, 153.43, 148.98, 147.46, 142.53, 141.15, 137.10, 133.24, 132.77, 130.39, 129.55, 125.40, 124.97, 120.20, 119.38, 115.85, 111.63, 111.34, 104.88, 77.23, 60.79, 55.95, 55.91, 55.88, 52.80, 50.76, 44.08, 38.45, 31.59, 29.71, 27.08, 25.09, 20.63.

2-(3-((R)-1-(((S)-1-((S)-2-(5-Bromothiophen-2-yl)-2-(3,4,5-trimethoxyphenyl)-acetyl)-piperidine-2-carbonyloxy)-3-(3,4-dimethoxyphenyl)propyl)phenoxy)-acetic acid (17f)

Following the general procedure B compound **17f** was synthesized using: Resin **5** (208 mg, 0.09 mmol, 1.10 eq., loading: 0.45 mmol/g), **16f** (33 mg, 0.09 mmol, 1.00 eq.), oxalyl chloride (15 μL, 0.17 mmol, 2.00 eq.), DIPEA (74 μL, 0.43 mmol, 5.00 eq.) and 0.47 mL DCM. After purification via preparative HPLC (50 - 80%, solvent B), compound **17f** (11 mg, 14.04 μmol, 16%) was obtained as a white solid. HPLC (50 – 100 % solvent B, 3 min) R_t = 1.589 min, purity (220 nm): 99%. HRMS (ESI⁺): m/z: calculated 826.18912 [M+H]⁺, found 826.18954 [M+H]⁺. ¹H NMR (500 MHz, CDCl₃) δ 7.30 – 7.23 (m, 1H), 6.91 – 6.86 (m, 2H), 6.82 (d, J = 3.8 Hz, 1H), 6.80 – 6.77 (m, 2H), 6.70 – 6.63 (m, 3H), 6.50 (s, 2H), 5.69 (dd, J = 8.5, 5.2 Hz, 1H), 5.55 – 5.47 (m, 1H), 5.26 (s, 1H), 4.69 – 4.58 (m, 2H), 3.86 (s, 3H), 3.86 (s, 3H), 3.84 – 3.83 (m, 1H), 3.83 (s, 3H), 3.82 (s, 6H), 3.31 (td, J = 13.0, 2.7 Hz, 1H), 2.69 – 2.62 (m, 1H), 2.59 – 2.52 (m, 1H), 2.38 – 2.29 (m, 1H), 2.28 – 2.19 (m, 1H), 2.13 – 2.03 (m, 1H), 1.73 – 1.61 (m, 2H), 1.57 – 1.49 (m, 1H), 1.39 – 1.23 (m, 1H), 1.11 – 1.01 (m, 1H). ¹³C NMR (126 MHz, CDCl₃) δ 171.23, 170.95, 170.24, 158.03, 153.63, 149.06, 147.57, 143.45, 142.13, 137.69, 134.04, 133.44, 129.94, 129.17, 126.84, 120.35, 119.82, 115.68, 112.57, 111.85, 111.52, 110.46, 105.49, 76.76, 65.36, 61.04, 56.42, 56.05, 53.10, 50.98, 44.23, 38.17, 31.58, 27.14, 25.02, 20.88.

2-(3-((R)-3-(3,4-Dimethoxyphenyl)-1-(((S)-1-((S)-2-(5-ethylthiophen-2-yl)-2-(3,4,5-trimethoxyphenyl)acetyl)piperidine-2-carbonyloxy)propyl)phenoxy)acetic acid (17g)

Following the general procedure C compound **17g** was synthesized using: Resin **5** (291 mg, 0.13 mmol, 1.10 eq., loading: 0.45 mmol/g), **16g** (40 mg, 0.12 mmol, 1.00 eq.), oxalyl chloride (20 μL, 0.24 mmol, 2.00 eq.), DIPEA (104 μL, 0.59 mmol, 5.00 eq.) and 0.48 mL DCM. After purification via preparative HPLC (50 - 80%, solvent B) compound **17g** (23 mg, 29.67 μmol, 25%) was

obtained as a white solid. HPLC (50 – 100 % solvent B, 3 min) R_t = 1.604 min, purity (220 nm): 99%. HRMS (ESI⁺): m/z: calculated 776.30991 [M+H]⁺, found 776.31047 [M+H]⁺. ¹H NMR (500 MHz, CDCl₃) δ 7.21 (t, J = 7.9 Hz, 1H), 6.87 – 6.83 (m, 1H), 6.79 (dd, J = 7.8, 6.2 Hz, 2H), 6.74 (t, J = 1.8 Hz, 1H), 6.71 – 6.66 (m, 2H), 6.63 (d, J = 3.5 Hz, 1H), 6.60 – 6.57 (m, 1H), 6.35 (s, 2H), 5.54 (dd, J = 8.9, 4.7 Hz, 1H), 5.50 – 5.47 (m, 1H), 5.32 (s, 1H), 4.71 – 4.56 (m, 2H), 3.86 (s, 3H), 3.85 (s, 3H), 3.85 – 3.81 (m, 1H), 3.78 (s, 3H), 3.56 (s, 6H), 3.14 (td, J = 13.3, 3.1 Hz, 1H), 2.81 – 2.73 (m, 2H), 2.72 – 2.65 (m, 1H), 2.61 – 2.51 (m, 1H), 2.36 – 2.30 (m, 1H), 2.24 – 2.15 (m, 1H), 2.08 – 1.96 (m, 1H), 1.86 – 1.73 (m, 2H), 1.68 – 1.64 (m, 1H), 1.50 – 1.38 (m, 1H), 1.37 – 1.29 (m, 1H), 1.25 (t, J = 7.5 Hz, 3H). ¹³C NMR (126 MHz, CDCl₃) δ 172.18, 171.13, 170.39, 158.19, 153.36, 149.08, 148.09, 147.55, 142.60, 139.29, 136.96, 133.74, 133.42, 129.69, 126.20, 122.45, 120.34, 119.51, 115.76, 111.78, 111.48, 109.19, 105.32, 76.91, 56.07, 56.02, 55.98.

2-(3-((R)-1-(((S)-1-((S)-2-(5-Cyclopropylthiophen-2-yl)-2-(3,4,5-trimethoxyphenyl)-acetyl)-piperidine-2-carbonyloxy)-3-(3,4-dimethoxyphenyl)propyl)phenoxy)-acetic acid (17h)

Following the general procedure C compound **17h** was synthesized using: Resin **5** (316 mg, 0.14 mmol, 1.10 eq., loading: 0.45 mmol/g), **16h** (45 mg, 0.13 mmol, 1.00 eq.), oxalyl chloride (22 μ L, 0.26 mmol, 2.00 eq.), DIPEA (112 μ L, 0.65 mmol, 5.00 eq.) and 1.29 mL DCM. After purification via preparative HPLC (50 - 80%, solvent B) compound **17h** (32 mg, 40.61 μ mol, 31%) was obtained as a white solid. HPLC (50 – 100 % solvent B, 3 min) R_t = 1.613 min, purity (220 nm): 98%. HRMS (ESI⁺): m/z: calculated 788.30991 [M+H]⁺, found 788.30977 [M+H]⁺. ¹H NMR (500 MHz, CDCl₃) δ 7.21 (t, J = 7.9 Hz, 1H), 6.85 (dd, J = 8.3, 2.4 Hz, 1H), 6.79 (dd, J = 7.8, 5.8 Hz, 2H), 6.73 (t, J = 1.8 Hz, 1H), 6.68 (d, J = 9.1 Hz, 2H), 6.60 (d, J = 3.5 Hz, 1H), 6.55 (d, J = 3.5 Hz, 1H), 6.33 (s, 2H), 5.79 (s, 1H), 5.54 (dd, J = 9.0, 4.7 Hz, 1H), 5.47 (d, J = 5.7 Hz, 1H), 5.29 (s, 1H), 4.70 – 4.53 (m, 2H), 3.86 (s, 3H), 3.85 (s, 3H), 3.83 (d, J = 8.0 Hz, 1H), 3.78 (s, 3H), 3.55 (s, 6H), 3.13 (td, J = 13.4, 3.1 Hz, 1H), 2.71 – 2.62 (m, 1H), 2.61 – 2.49 (m, 1H), 2.36 – 2.29 (m, 1H), 2.24 – 2.14 (m, 1H), 2.07 – 1.94 (m, 2H), 1.84 – 1.74 (m, 2H), 1.69 – 1.64 (m, 1H), 1.46 – 1.26 (m, 2H), 0.95 – 0.86 (m, 2H), 0.70 – 0.64 (m, 2H). ¹³C NMR (126 MHz, CDCl₃) δ 172.12, 171.18, 170.39, 158.19, 153.35, 149.17, 149.07, 147.55, 142.60, 138.54, 136.97, 133.68, 133.42, 129.69, 126.18, 121.78, 120.34, 119.51, 115.76, 111.77, 111.48, 109.22, 109.22, 105.31, 105.31, 77.37, 65.45, 60.90, 56.07, 56.02, 55.99, 52.86, 50.45, 44.12, 38.54, 31.67, 27.16, 25.18, 20.76, 11.29, 9.71, 9.67.

2-(3-((R)-1-(((S)-1-((S)-2-(5-cyanothiophen-2-yl)-2-(3,4,5-trimethoxyphenyl)-acetyl)-piperidine-2-carbonyloxy)-3-(3,4-dimethoxyphenyl)propyl)phenoxy)-acetic acid (17i)

A 10 mL filter syringe was charged with resin **5** (225 mg, 0.06 mmol, 0.50 eq., loading: 0.30 mmol/g), and the resin was swelled for 10 min in DCM. After filtration, the resin was washed with DMF and treated three times with a pre-cooled solution of 20 vol.-% 4-methylpiperidine in DMF for 5 min. After complete Fmoc deprotection, the resin was filtered and washed twice with DMF, followed by DCM. The obtained resin was then treated with a solution containing **16i** (45 mg, 0.12 mmol, 1.00 eq.), TCFH (45 mg, 0.14 mmol, 1.20 eq.), and NMI (38 μ L, 0.42 mmol, 3.50 eq.) in 0.67 mL DCM/ACN (1:1) at rt overnight. After the complete conversion of the starting material, the resin was filtered and washed twice with DCM. Finally, the product was cleaved off the resin by treating it with a solution of 20 vol.-% HFIP in DCM for 1 h. After removal of the solvent under reduced pressure and purification via preparative HPLC. The respective compounds were obtained as white solids. After purification via preparative HPLC (50 - 80%, solvent B), compound **17i** (11 mg, 14.23 μ mol, 21%) was obtained as a pale-yellow solid. HPLC (30 – 100 % solvent B, 3 min) R_t = 1.846 min, purity (220 nm): 99%. HRMS (ESI⁺): m/z: calculated 773.2739 [M+H]⁺, found 773.2742 [M+H]⁺. ¹H NMR (500 MHz, CDCl₃) δ 7.41 (d, J = 3.8 Hz, 1H), 7.22 (t, J = 7.9 Hz, 1H), 6.88 – 6.85 (m, 2H), 6.81 – 6.76 (m, 2H), 6.76 – 6.73 (m, 1H), 6.69 – 6.65 (m, 2H), 6.33 (s, 2H), 5.52 (dd, J = 8.9, 4.8 Hz, 1H), 5.45 – 5.41 (m, 1H), 5.39 (s, 1H), 4.73 – 4.63 (m, 2H), 3.86 (s, 3H), 3.85 (s, 3H), 3.78 (s, 3H), 3.74 – 3.69 (m, 1H), 3.54 (s, 6H), 3.07 (td, J = 13.5, 3.2 Hz, 1H), 2.72 – 2.64 (m, 1H), 2.62 – 2.53 (m, 1H), 2.40 – 2.34 (m, 1H), 2.23 – 2.15 (m, 1H), 2.07 – 1.96 (m, 1H), 1.87 – 1.74 (m, 2H), 1.74 – 1.67 (m, 1H), 1.56 – 1.45 (m, 1H), 1.38 – 1.23 (m, 1H). ¹³C NMR (126 MHz, CDCl₃) δ 171.03, 170.32, 170.01, 158.20, 153.80, 151.07, 149.12, 147.62, 142.58, 137.57, 136.67, 133.33, 132.13, 129.74, 126.71, 120.34, 119.49, 115.87, 114.57, 111.77, 111.48, 110.05, 108.99, 104.93, 77.20, 65.38, 60.93, 56.08, 56.05, 56.04, 52.98, 50.78, 44.29, 38.58, 31.69, 27.17, 25.21, 20.71.

(S)-(R)-3-(3,4-Dimethoxyphenyl)-1-(3-(2-morpholinoethoxy)phenyl)propyl-1-((S)-2-(5-methylthiophen-2-yl)-2-(3,4,5-trimethoxyphenyl)acetyl)piperidine-2-carboxylate (19a)

In a 10 mL flask, **16e** (40 mg, 0.12 mmol, 1.00 eq) and amine **18** (70 mg, 0.15 mmol, 1.10 eq.) were dissolved in 1.24 mL MeCN. Then NMI (35 μ L, 0.43 mmol, 3.50 eq.) was added, followed by TCFH (42 mg, 0.15 mmol, 1.20 eq.). The resulting solution was stirred at rt overnight. After

the complete conversion of **18**, the solvent was removed under reduced pressure. After purification via preparative HPLC (5 - 80%, solvent B), compound **19e** (21 mg, 25 μ mol, 20%) was obtained as a white solid. HPLC (5 - 100 % solvent B, 3 min) R_t = 1.969 min, purity (220 nm): 99%. HRMS (ESI⁺): m/z: calculated 817.37284 [M+H]⁺, found 817.37304 [M+H]⁺. ¹H NMR (500 MHz, CDCl₃) δ 7.19 (t, J = 7.9 Hz, 1H), 6.82 (t, J = 2.0 Hz, 1H), 6.81 - 6.75 (m, 3H), 6.66 (dd, J = 8.2, 2.2 Hz, 1H), 6.64 - 6.62 (m, 2H), 6.57 - 6.53 (m, 1H), 6.46 (s, 2H), 5.65 (dd, J = 8.2, 5.4 Hz, 1H), 5.52 - 5.44 (m, 1H), 5.32 (s, 1H), 4.11 (t, J = 5.7 Hz, 2H), 3.85 (s, 6H), 3.79 (s, 3H), 3.74 (t, J = 4.7 Hz, 4H), 3.67 (s, 6H), 3.11 (td, J = 13.1, 3.1 Hz, 1H), 2.81 (t, J = 5.6 Hz, 2H), 2.64 - 2.55 (m, 5H), 2.56 - 2.46 (m, 1H), 2.42 (s, 3H), 2.35 - 2.29 (m, 1H), 2.17 (dtd, J = 14.1, 8.9, 5.6 Hz, 1H), 2.06 - 1.95 (m, 1H), 1.78 - 1.70 (m, 2H), 1.67 - 1.56 (m, 2H), 1.39 - 1.17 (m, 2H). ¹³C NMR (126 MHz, CDCl₃) δ 171.21, 170.67, 158.88, 153.34, 149.02, 147.49, 141.92, 140.36, 140.29, 137.08, 134.38, 133.59, 129.70, 126.05, 124.26, 120.27, 118.79, 114.05, 111.82, 111.43, 105.52, 76.36, 66.89, 65.65, 60.88, 57.73, 56.08, 56.06, 55.98, 54.13, 52.59, 50.27, 44.03, 38.38, 31.50, 26.96, 25.32, 20.98, 15.48.

(S)-(R)-3-(3,4-Dimethoxyphenyl)-1-(3-(2-morpholinoethoxy)phenyl)propyl-1-((S)-2-(5-chlorothiophen-2-yl)-2-(3,4,5-trimethoxyphenyl)acetyl)piperidine-2-carboxylate (19b)

In a 4 mL vial, **16f** (40 mg, 0.12 mmol, 1.00 eq) was dissolved in 1 mL DCM, and the solution was cooled to 0°C. Then oxalyl chloride (90 μ L, 0.18 mmol, 1.50 eq.) was added, followed by a drop of DMF, and the mixture was stirred for 1h at rt. After the complete formation of the acid chloride, the solvent was removed under reduced pressure. In a second flask, amine **18** (66 mg, 0.13 mmol, 1.10 eq.) and DIPEA (60 μ L, 0.35 mmol, 3.00 eq.) were dissolved in 0.70 mL DCM, and the resulting solution was cooled to 0°C. Then the acid chloride was added dropwise as a solution in DCM. The reaction mixture was then stirred at rt for 1h. Then the solvent was removed under reduced pressure, the crude product was purified directly via preparative HPLC (5 - 80%, solvent B), and compound **19f** (17 mg, 20 μ mol, 17%) was obtained as a white solid. HPLC (5 - 100 % solvent B, 3 min) R_t = 1.995 min, purity (220 nm): 99%. HRMS (ESI⁺): m/z: calculated 837.31822 [M+H]⁺, found 837.31853 [M+H]⁺. ¹H NMR (500 MHz, CDCl₃) δ 7.19 (t, J = 7.9 Hz, 1H), 6.90 - 6.74 (m, 4H), 6.71 (d, J = 3.7 Hz, 1H), 6.69 - 6.60 (m, 3H), 6.42 (s, 2H), 5.63 (dd, J = 8.2, 5.3 Hz, 1H), 5.44 - 5.40 (m, 1H), 5.29 (s, 1H), 4.19 - 4.05 (m, 2H), 3.85 (s, 6H), 3.79 (s, 3H), 3.77 - 3.71 (m, 4H), 3.65 (s, 6H), 3.07 (td, J = 13.3, 3.1 Hz, 1H), 2.82 (t, J = 6.1 Hz, 2H), 2.68 -

2.56 (m, 4H), 2.54 – 2.46 (m, 2H), 2.37 – 2.26 (m, 1H), 2.22 – 2.10 (m, 1H), 2.08 – 1.95 (m, 1H), 1.80 – 1.71 (m, 2H), 1.69 – 1.57 (m, 1H), 1.50 – 1.40 (m, 1H), 1.36 – 1.24 (m, 2H). ¹³C NMR (126 MHz, CDCl₃) δ 170.64, 170.54, 158.94, 153.54, 149.04, 147.52, 141.90, 141.86, 137.31, 133.56, 133.48, 130.43, 129.69, 125.17, 124.91, 120.28, 118.70, 114.13, 112.52, 111.81, 111.44, 105.21, 76.48, 66.94, 60.91, 57.79, 56.11, 56.07, 55.99, 54.17, 52.67, 50.67, 44.10, 38.40, 31.53, 26.94, 25.31, 20.89.

ASSOCIATED CONTENT

Supporting Information.

Further experimental details: crystallographic data collection and refinement statistics, X-ray structures, additional synthetic representations and explanations, analytical data of intermediate compounds, additional information and binding curves from FP assay, NMR spectra and HPLC traces of final compounds (PDF). Molecular formula strings (CSV).

Accession Codes. Atomic coordinates for the X-ray structures of compounds **(S)-9**, **(S)-13a**, **(S)-13b**, **(S)-13c** and **17e** are available from the RCSB Protein Data Bank (www.rcsb.org). The authors will release the atomic coordinates and experimental data upon article publication.

AUTHOR INFORMATION

Corresponding Author

*Phone: +49-6151-16-21245. E-mail: felix.hausch@tu-darmstadt.de

ORCID

Felix Hausch: 0000-0002-3710-8838

Funding Sources

This work was supported by the VIP+ grant Fit4Fat (03VP08671), the LOEWE cluster TRABITA, and the BMBF grant 51TaVAIP (16GW0290).

ACKNOWLEDGMENT

Diffraction data have been collected on BL14.1 at the BESSY II electron storage ring operated by the Helmholtz-Zentrum Berlin, Germany. We thank HZB for the allocation of synchrotron radiation beamtime and we would particularly like to acknowledge the help and support of Manfred Weiss and the whole MX team during the experiment.

ABBREVIATIONS

COMU (1-Cyano-2-ethoxy-2-oxoethylideneaminoxy)dimethylamino-morpholino-carbenium-hexafluorophosphate, HATU [O-(7-Azabenzotriazol-1-yl)-N,N,N',N'-tetramethyluronium-hexafluorophosphate], HFIP 1,1,1,3,3,3-Hexafluoroisopropanol, HOAt 1-Hydroxy-7-azabenzotriazole, TCFH Chloro-N,N,N',N'-tetramethylformamidinium hexafluorophosphate, NMI 1-methylimidazole, T3P Propylphosphonic anhydride,

REFERENCES

- (1) Sinars, C. R.; Cheung-Flynn, J.; Rimerman, R. A.; Scammell, J. G.; Smith, D. F.; Clardy, J. Structure of the Large FK506-Binding Protein FKBP51, an Hsp90-Binding Protein and a Component of Steroid Receptor Complexes. *Proceedings of the National Academy of Sciences* **2003**, *100* (3), 868–873. <https://doi.org/10.1073/pnas.0231020100>.
- (2) Cheung-Flynn, J.; Roberts, P. J.; Riggs, D. L.; Smith, D. F. C-Terminal Sequences Outside the Tetratricopeptide Repeat Domain of FKBP51 and FKBP52 Cause Differential Binding to Hsp90. *Journal of Biological Chemistry* **2003**, *278* (19), 17388–17394. <https://doi.org/10.1074/jbc.M300955200>.
- (3) Wochnik, G. M.; Rüegg, J.; Abel, G. A.; Schmidt, U.; Holsboer, F.; Rein, T. FK506-Binding Proteins 51 and 52 Differentially Regulate Dynein Interaction and Nuclear Translocation of the Glucocorticoid Receptor in Mammalian Cells. *Journal of Biological Chemistry* **2005**, *280* (6), 4609–4616. <https://doi.org/10.1074/jbc.M407498200>.
- (4) Binder, E. B. The Role of FKBP5, a Co-Chaperone of the Glucocorticoid Receptor in the Pathogenesis and Therapy of Affective and Anxiety Disorders. *Psychoneuroendocrinology* **2009**, *34*, S186–S195. <https://doi.org/10.1016/j.psyneuen.2009.05.021>.
- (5) Storer, C. L.; Dickey, C. A.; Galigniana, M. D.; Rein, T.; Cox, M. B. FKBP51 and FKBP52 in Signaling and Disease. *Trends in Endocrinology & Metabolism* **2011**, *22* (12), 481–490. <https://doi.org/10.1016/j.tem.2011.08.001>.
- (6) Sanchez, E. R. Chaperoning Steroidal Physiology: Lessons from Mouse Genetic Models of Hsp90 and Its Cochaperones. *Biochimica et Biophysica Acta (BBA) - Molecular Cell Research* **2012**, *1823* (3), 722–729. <https://doi.org/10.1016/j.bbamcr.2011.11.006>.
- (7) O’Leary, J. C.; Dharia, S.; Blair, L. J.; Brady, S.; Johnson, A. G.; Peters, M.; Cheung-Flynn, J.; Cox, M. B.; de Erausquin, G.; Weeber, E. J.; Jinwal, U. K.; Dickey, C. A. A New Anti-Depressive Strategy for the Elderly: Ablation of FKBP5/FKBP51. *PLoS One* **2011**, *6* (9), e24840. <https://doi.org/10.1371/journal.pone.0024840>.
- (8) Touma, C.; Gassen, N. C.; Herrmann, L.; Cheung-Flynn, J.; Büll, D. R.; Ionescu, I. A.; Heinzmann, J.-M.; Knapman, A.; Siebertz, A.; Depping, A.-M.; Hartmann, J.; Hausch, F.; Schmidt, M. v.; Holsboer, F.; Ising, M.; Cox, M. B.; Schmidt, U.; Rein, T. FK506 Binding Protein 5 Shapes Stress Responsiveness: Modulation of Neuroendocrine Reactivity and Coping Behavior. *Biol Psychiatry* **2011**, *70* (10), 928–936. <https://doi.org/10.1016/j.biopsych.2011.07.023>.
- (9) Hartmann, J.; Wagner, K. v.; Liebl, C.; Scharf, S. H.; Wang, X.-D.; Wolf, M.; Hausch, F.; Rein, T.; Schmidt, U.; Touma, C.; Cheung-Flynn, J.; Cox, M. B.; Smith, D. F.; Holsboer, F.; Müller, M. B.; Schmidt, M. v. The Involvement of FK506-Binding Protein 51 (FKBP5) in the Behavioral and Neuroendocrine Effects of Chronic Social Defeat Stress. *Neuropharmacology* **2012**, *62* (1), 332–339. <https://doi.org/10.1016/j.neuropharm.2011.07.041>.

- (10) Albu, S.; Romanowski, C. P. N.; Letizia Curzi, M.; Jakubcakova, V.; Flachskamm, C.; Gassen, N. C.; Hartmann, J.; Schmidt, M. v.; Schmidt, U.; Rein, T.; Holsboer, F.; Hausch, F.; Paez-Pereda, M.; Kimura, M. Deficiency of FK506-Binding Protein (FKBP) 51 Alters Sleep Architecture and Recovery Sleep Responses to Stress in Mice. *J Sleep Res* **2014**, *23* (2), 176–185. <https://doi.org/10.1111/jsr.12112>.
- (11) Balsevich, G.; Häusl, A. S.; Meyer, C. W.; Karamihalev, S.; Feng, X.; Pöhlmann, M. L.; Dournes, C.; Uribe-Marino, A.; Santarelli, S.; Labermaier, C.; Hafner, K.; Mao, T.; Breitsamer, M.; Theodoropoulou, M.; Namendorf, C.; Uhr, M.; Paez-Pereda, M.; Winter, G.; Hausch, F.; Chen, A.; Tschöp, M. H.; Rein, T.; Gassen, N. C.; Schmidt, M. v. Stress-Responsive FKBP51 Regulates AKT2-AS160 Signaling and Metabolic Function. *Nat Commun* **2017**, *8* (1), 1725. <https://doi.org/10.1038/s41467-017-01783-y>.
- (12) Sidibeh, C. O.; Pereira, M. J.; Abalo, X. M.; J. Boersma, G.; Skrtic, S.; Lundkvist, P.; Katsogiannos, P.; Hausch, F.; Castillejo-López, C.; Eriksson, J. W. FKBP5 Expression in Human Adipose Tissue: Potential Role in Glucose and Lipid Metabolism, Adipogenesis and Type 2 Diabetes. *Endocrine* **2018**, *62* (1), 116–128. <https://doi.org/10.1007/s12020-018-1674-5>.
- (13) Pereira, M. J.; Palming, J.; Svensson, M. K.; Rizell, M.; Dalenbäck, J.; Hammar, M.; Fall, T.; Sidibeh, C. O.; Svensson, P.-A.; Eriksson, J. W. FKBP5 Expression in Human Adipose Tissue Increases Following Dexamethasone Exposure and Is Associated with Insulin Resistance. *Metabolism* **2014**, *63* (9), 1198–1208. <https://doi.org/10.1016/j.metabol.2014.05.015>.
- (14) Linnstaedt, S. D.; Riker, K. D.; Rueckeis, C. A.; Kutchko, K. M.; Lackey, L.; McCarthy, K. R.; Tsai, Y.-H.; Parker, J. S.; Kurz, M. C.; Hendry, P. L.; Lewandowski, C.; Datner, E.; Pearson, C.; O’Neil, B.; Domeier, R.; Kaushik, S.; Laederach, A.; McLean, S. A. A Functional RiboSNitch in the 3’ Untranslated Region of *FKBP5* Alters MicroRNA-320a Binding Efficiency and Mediates Vulnerability to Chronic Post-Traumatic Pain. *The Journal of Neuroscience* **2018**, *38* (39), 8407–8420. <https://doi.org/10.1523/JNEUROSCI.3458-17.2018>.
- (15) Wanstrath, B. J.; McLean, S. A.; Zhao, Y.; Mickelson, J.; Bauder, M.; Hausch, F.; Linnstaedt, S. D. Duration of Reduction in Enduring Stress-Induced Hyperalgesia Via FKBP51 Inhibition Depends on Timing of Administration Relative to Traumatic Stress Exposure. *J Pain* **2022**, *23* (7), 1256–1267. <https://doi.org/10.1016/j.jpain.2022.02.007>.
- (16) Wedel, S.; Mathoor, P.; Rauh, O.; Heymann, T.; Ciotu, C. I.; Fuhrmann, D. C.; Fischer, M. J. M.; Weigert, A.; de Bruin, N.; Hausch, F.; Geisslinger, G.; Sisignano, M. SAFit2 Reduces Neuroinflammation and Ameliorates Nerve Injury-Induced Neuropathic Pain. *Journal of Neuroinflammation* **2022**, *19*:1 **2022**, *19* (1), 1–21. <https://doi.org/10.1186/S12974-022-02615-7>.
- (17) Schmidt, M. v.; Paez-Pereda, M.; Holsboer, F.; Hausch, F. The Prospect of FKBP51 as a Drug Target. *ChemMedChem* **2012**, *7* (8), 1351–1359. <https://doi.org/10.1002/cmde.201200137>.

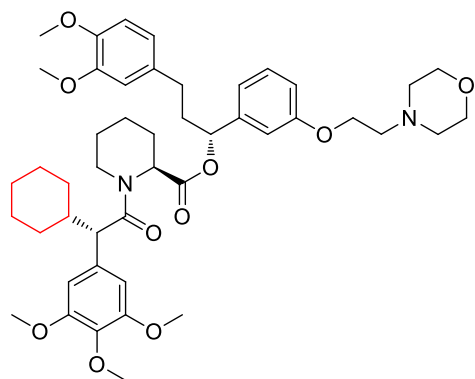
- (18) Hausch, F. FKBP5s and Their Role in Neuronal Signaling. *Biochimica et Biophysica Acta (BBA) - General Subjects* **2015**, *1850* (10), 2035–2040. <https://doi.org/10.1016/j.bbagen.2015.01.012>.
- (19) Fries, G.; Gassen, N.; Rein, T. The FKBP51 Glucocorticoid Receptor Co-Chaperone: Regulation, Function, and Implications in Health and Disease. *Int J Mol Sci* **2017**, *18* (12), 2614. <https://doi.org/10.3390/ijms18122614>.
- (20) Gopalakrishnan, R.; Kozany, C.; Gaali, S.; Kress, C.; Hoogeland, B.; Bracher, A.; Hausch, F. Evaluation of Synthetic FK506 Analogues as Ligands for the FK506-Binding Proteins 51 and 52. *J Med Chem* **2012**, *55* (9), 4114–4122. <https://doi.org/https://doi.org/10.1021/jm201746x>.
- (21) Gopalakrishnan, R.; Kozany, C.; Wang, Y.; Schneider, S.; Hoogeland, B.; Bracher, A.; Hausch, F. Exploration of Pipecolate Sulfonamides as Binders of the FK506-Binding Proteins 51 and 52. *J Med Chem* **2012**, *55* (9), 4123–4131. <https://doi.org/https://doi.org/10.1021/jm201747c>.
- (22) Riggs, D. L.; Roberts, P. J.; Chirillo, S. C.; Cheung-Flynn, J.; Prapapanich, V.; Ratajczak, T.; Gaber, R.; Picard, D.; Smith, D. F. The Hsp90-Binding Peptidylprolyl Isomerase FKBP52 Potentiates Glucocorticoid Signaling in Vivo. *EMBO J* **2003**, *22* (5), 1158–1167. <https://doi.org/10.1093/emboj/cdg108>.
- (23) Gaali, S.; Feng, X.; Hähle, A.; Sippel, C.; Bracher, A.; Hausch, F. Rapid, Structure-Based Exploration of Pipecolic Acid Amides as Novel Selective Antagonists of the FK506-Binding Protein 51. *J Med Chem* **2016**, *59* (6), 2410–2422. <https://doi.org/https://doi.org/10.1021/acs.jmedchem.5b01355>.
- (24) Gaali, S.; Kirschner, A.; Cuboni, S.; Hartmann, J.; Kozany, C.; Balsevich, G.; Namendorf, C.; Fernandez-Vizarra, P.; Sippel, C.; Zannas, A. S.; Draenert, R.; Binder, E. B.; Almeida, O. F. X.; Rühler, G.; Uhr, M.; Schmidt, M. v.; Touma, C.; Bracher, A.; Hausch, F. Selective Inhibitors of the FK506-Binding Protein 51 by Induced Fit. *Nature Chemical Biology* **2014**, *11:1* **2014**, *11* (1), 33–37. <https://doi.org/10.1038/nchembio.1699>.
- (25) Feng, X.; Sippel, C.; Bracher, A.; Hausch, F. Structure-Affinity Relationship Analysis of Selective FKBP51 Ligands. *J Med Chem* **2015**, *58* (19), 7796–7806. <https://doi.org/https://doi.org/10.1021/acs.jmedchem.5b00785>.
- (26) Bauder, M.; Meyners, C.; Purder, P. L.; Merz, S.; Sugiarto, W. O.; Voll, A. M.; Heymann, T.; Hausch, F. Structure-Based Design of High-Affinity Macrocyclic FKBP51 Inhibitors. *J Med Chem* **2021**, *64* (6), 3320–3349. https://doi.org/10.1021/ACS.JMEDCHEM.0C02195/SUPPL_FILE/JM0C02195_SI_002.CSV.
- (27) Feng, X.; Sippel, C.; Knaup, F. H.; Bracher, A.; Staibano, S.; Romano, M. F.; Hausch, F. A Novel Decalin-Based Bicyclic Scaffold for FKBP51-Selective Ligands. *J Med Chem* **2020**, *63* (1), 231–240. <https://doi.org/https://doi.org/10.1021/acs.jmedchem.9b01157>.

- (28) Voll, A. M.; Meyners, C.; Taubert, M. C.; Bajaj, T.; Heymann, T.; Merz, S.; Charalampidou, A.; Kolos, J.; Purder, P. L.; Geiger, T. M.; Wessig, P.; Gassen, N. C.; Bracher, A.; Hausch, F. Macrocyclic FKBP51 Ligands Define a Transient Binding Mode with Enhanced Selectivity. *Angewandte Chemie International Edition* **2021**, *60* (24), 13257–13263. <https://doi.org/10.1002/ANIE.202017352>.
- (29) Gabani, B. B.; Sulochana, S. P.; Siddesh, A. H. A.; Kiran, V.; Saini, N. K.; Samanta, S. K.; Hallur, M. S.; Rajagopal, S.; Mullangi, R. Validated LC-MS/MS Method for Simultaneous Quantitation of SAFit-1 and SAFit-2 in Mice Plasma: Application to a Pharmacokinetic Study. *Drug Res* **2020**, *70* (07), 325–332. <https://doi.org/10.1055/a-1164-6123>.
- (30) Bracher, A.; Kozany, C.; Thost, A. K.; Hausch, F. Structural Characterization of the PPIase Domain of FKBP51, a Cochaperone of Human Hsp90. *Acta Crystallogr. D Biol Crystallogr.* **2011**, *67* (6), 549–559. <https://doi.org/10.1107/S0907444911013862>.
- (31) Kozany, C.; März, A.; Kress, C.; Hausch, F. Fluorescent Probes to Characterise FK506-Binding Proteins. *ChemBioChem* **2009**, *10* (8), 1402–1410. <https://doi.org/10.1002/CBIC.200800806>.
- (32) Gnatzy, M. T.; Geiger, T. M.; Kuehn, A.; Gutfreund, N.; Walz, M.; Kolos, J. M.; Hausch, F. Development of NanoBRET-Binding Assays for FKBP-Ligand Profiling in Living Cells. *ChemBioChem* **2021**, *22* (13), 2257–2261. <https://doi.org/10.1002/cbic.202100113>.
- (33) Maiarù, M.; Tochiki, K. K.; Cox, M. B.; Annan, L. v.; Bell, C. G.; Feng, X.; Hausch, F.; Géranton, S. M. The Stress Regulator FKBP51 Drives Chronic Pain by Modulating Spinal Glucocorticoid Signaling. *Sci Transl Med* **2016**, *8* (325). <https://doi.org/https://doi.org/10.1126/scitranslmed.aab3376>.
- (34) Maiarù, M.; Morgan, O. B.; Mao, T.; Breitsamer, M.; Bamber, H.; Pöhlmann, M.; Schmidt, M. v.; Winter, G.; Hausch, F.; Géranton, S. M. The Stress Regulator FKBP51: A Novel and Promising Druggable Target for the Treatment of Persistent Pain States across Sexes. *Pain* **2018**, *159* (7), 1224–1234. <https://doi.org/10.1097/J.PAIN.0000000000001204>.
- (35) Gerlach, M.; Mueller, U.; Weiss, M. S. The MX Beamlines BL14.1-3 at BESSY II. *Journal of large-scale research facilities JLSRF* **2016**, *2*, A47. <https://doi.org/10.17815/jlsrf-2-64>.
- (36) Collaborative Computational Project, N. 4. The CCP4 Suite: Programs for Protein Crystallography. *Acta Crystallogr D Biol Crystallogr* **1994**, *50* (5), 760–763. <https://doi.org/10.1107/S0907444994003112>.
- (37) Potterton, E.; Briggs, P.; Turkenburg, M.; Dodson, E. A Graphical User Interface to the CCP 4 Program Suite. *Acta Crystallogr D Biol Crystallogr* **2003**, *59* (7), 1131–1137. <https://doi.org/10.1107/S0907444903008126>.
- (38) Winter, G.; Waterman, D. G.; Parkhurst, J. M.; Brewster, A. S.; Gildea, R. J.; Gerstel, M.; Fuentes-Montero, L.; Vollmar, M.; Michels-Clark, T.; Young, I. D.; Sauter, N. K.; Evans, G. DIALS: Implementation and Evaluation of a New Integration Package. *Acta Crystallogr D Struct Biol* **2018**, *74* (2), 85–97. <https://doi.org/10.1107/S2059798317017235>.

- (39) Potterton, L.; Agirre, J.; Ballard, C.; Cowtan, K.; Dodson, E.; Evans, P. R.; Jenkins, H. T.; Keegan, R.; Krissinel, E.; Stevenson, K.; Lebedev, A.; McNicholas, S. J.; Nicholls, R. A.; Noble, M.; Pannu, N. S.; Roth, C.; Sheldrick, G.; Skubak, P.; Turkenburg, J.; Uski, V.; von Delft, F.; Waterman, D.; Wilson, K.; Winn, M.; Wojdyr, M. CCP4i2: The New Graphical User Interface to the CCP4 Program Suite. *Acta Crystallogr D Struct Biol* **2018**, *74* (2), 68–84. <https://doi.org/10.1107/S2059798317016035>.
- (40) Winn, M. D.; Ballard, C. C.; Cowtan, K. D.; Dodson, E. J.; Emsley, P.; Evans, P. R.; Keegan, R. M.; Krissinel, E. B.; Leslie, A. G. W.; McCoy, A.; McNicholas, S. J.; Murshudov, G. N.; Pannu, N. S.; Potterton, E. A.; Powell, H. R.; Read, R. J.; Vagin, A.; Wilson, K. S. Overview of the CCP 4 Suite and Current Developments. *Acta Crystallogr D Biol Crystallogr* **2011**, *67* (4), 235–242. <https://doi.org/10.1107/S0907444910045749>.
- (41) Evans, P. R.; Murshudov, G. N. How Good Are My Data and What Is the Resolution? *Acta Crystallogr D Biol Crystallogr* **2013**, *69* (7), 1204–1214. <https://doi.org/10.1107/S0907444913000061>.
- (42) Evans, P. R. An Introduction to Data Reduction: Space-Group Determination, Scaling and Intensity Statistics. *Acta Crystallogr D Biol Crystallogr* **2011**, *67* (4), 282–292. <https://doi.org/10.1107/S090744491003982X>.
- (43) McCoy, A. J.; Grosse-Kunstleve, R. W.; Adams, P. D.; Winn, M. D.; Storoni, L. C.; Read, R. J. Phaser Crystallographic Software. *J Appl Crystallogr* **2007**, *40* (4), 658–674. <https://doi.org/10.1107/S0021889807021206>.
- (44) Vagin, A. A.; Steiner, R. A.; Lebedev, A. A.; Potterton, L.; McNicholas, S.; Long, F.; Murshudov, G. N. REFMAC5 Dictionary: Organization of Prior Chemical Knowledge and Guidelines for Its Use. *Acta Crystallogr D Biol Crystallogr* **2004**, *60* (12), 2184–2195. <https://doi.org/10.1107/S0907444904023510>.
- (45) Winn, M. D.; Murshudov, G. N.; Papiz, M. Z. Macromolecular TLS Refinement in REFMAC at Moderate Resolutions; 2003; pp 300–321. [https://doi.org/10.1016/S0076-6879\(03\)74014-2](https://doi.org/10.1016/S0076-6879(03)74014-2).
- (46) Murshudov, G. N.; Vagin, A. A.; Dodson, E. J. Refinement of Macromolecular Structures by the Maximum-Likelihood Method. *Acta Crystallogr D Biol Crystallogr* **1997**, *53* (3), 240–255. <https://doi.org/10.1107/S0907444996012255>.
- (47) Nicholls, R. A.; Long, F.; Murshudov, G. N. Low-Resolution Refinement Tools in REFMAC5. *Acta Crystallogr D Biol Crystallogr* **2012**, *68* (4), 404–417. <https://doi.org/10.1107/S090744491105606X>.
- (48) Murshudov, G. N.; Skubák, P.; Lebedev, A. A.; Pannu, N. S.; Steiner, R. A.; Nicholls, R. A.; Winn, M. D.; Long, F.; Vagin, A. A. REFMAC5 for the Refinement of Macromolecular Crystal Structures. *Acta Crystallogr D Biol Crystallogr* **2011**, *67* (4), 355–367. <https://doi.org/10.1107/S0907444911001314>.

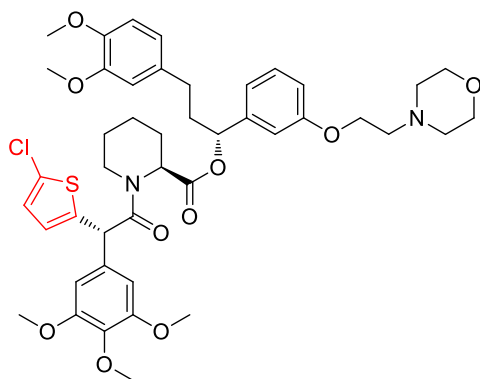
- (49) Emsley, P.; Lohkamp, B.; Scott, W. G.; Cowtan, K. Features and Development of Coot. *Acta Crystallogr D Biol Crystallogr* **2010**, *66* (4), 486–501. <https://doi.org/10.1107/S0907444910007493>.
- (50) van Aalten, D. M. F.; Bywater, R.; Findlay, J. B. C.; Hendlich, M.; Hooft, R. W. W.; Vriend, G. PRODRG, a Program for Generating Molecular Topologies and Unique Molecular Descriptors from Coordinates of Small Molecules. *J Comput Aided Mol Des* **1996**, *10* (3), 255–262. <https://doi.org/10.1007/BF00355047>.

Table of content



SAFit2

K_i (FKBP51) = 6 nM



19e

K_i (FKBP51) = 19 nM